



TITLE:

Microbial functions and soil nitrogen mineralisation processes in the soil of a cool temperate forest in northern Japan

AUTHOR(S):

Nakayama, Masataka; Imamura, Shihomi; Tatsumi, Chikae; Taniguchi, Takeshi; Tateno, Ryunosuke

CITATION:

Nakayama, Masataka ...[et al]. Microbial functions and soil nitrogen mineralisation processes in the soil of a cool temperate forest in northern Japan. *Biogeochemistry* 2021, 155(3): 359-379

ISSUE DATE:

2021-09

URL:

<http://hdl.handle.net/2433/269312>

RIGHT:

This version of the article has been accepted for publication, after peer review (when applicable) and is subject to Springer Nature's AM terms of use, but is not the Version of Record and does not reflect post-acceptance improvements, or any corrections. The Version of Record is available online at: <http://dx.doi.org/10.1007/s10533-021-00830-7>; The full-text file will be made open to the public on 12 July 2022 in accordance with publisher's 'Terms and Conditions for Self-Archiving'; This is not the published version. Please cite only the published version. この論文は出版社版ではありません。引用の際には出版社版をご確認ご利用ください。

1 (Authors)

2 Masataka Nakayama^a, Shihomi Imamura^a, Chikae Tatsumi^{a,b}, Takeshi Taniguchi^c, Ryunosuke
3 Tateno^d

4 (Title)

5 Microbial functions and soil nitrogen mineralisation processes in the soil of a cool temperate forest

6 in northern Japan

7

8 (The affiliations of the authors)

9 ^a *Graduate School of Agriculture, Kyoto University, Kyoto 606-8502, Japan*

10 ^b *Research Faculty of Agriculture, Hokkaido University, Hokkaido, 060-8589, Japan*

11 ^c *Arid Land Research Center, Tottori University, Tottori 680-0001, Japan*

12 ^d *Filed Science Education and Research Center, Kyoto University, Kyoto 606-8502, Japan*

13

14 (Corresponding Author)

15 Masataka Nakayama

16 Graduate School of Agriculture, Kyoto University, Kyoto 606-8502, Japan

17 Tel: +81-75-753-6440, Fax: +81-75-753-6443

18 E-mail: nakayama.masataka.32x@st.kyoto-u.ac.jp

19

20 (ORCID)

21 Masataka Nakayama: 0000-0003-3835-5512

22 Chikae Tatsumi: 0000-0001-7191-6049

23 Takeshi Taniguchi: 0000-0001-7386-1117

24 Ryunosuke Tateno: 0000-0001-8461-3696

25

26

27

28

29 **Abstract**

30

31 There is little knowledge about microbial functional community structures and the relationships
32 between microbial communities and nitrogen transformation processes. Here, we investigated the
33 relationships between soil microbial communities and nitrogen mineralisation potentials in a cool
34 temperate forest throughout the growing season. Microbial communities were assessed by
35 quantification of the total bacterial, archaeal, and fungal gene abundances and the bacterial and
36 archaeal amoA gene abundances, functional predictions of bacteria and fungi, and analysis of the
37 bacterial-fungal co-occurrence network. In mid-summer, ectomycorrhizal fungal abundance was
38 significantly higher, whereas the total bacterial abundance was significantly lower. Bacterial and
39 archaeal amoA gene abundances were also significantly higher in mid-summer. However, regardless
40 of the seasonal fluctuation of microbial gene abundances, the net nitrification and nitrogen
41 mineralisation potential did not show clear seasonality. In the network analysis, the microbial
42 community was divided into 13 modules, which were subgroups assumed to have similar niches.
43 Furthermore, two modules that mainly consisted of microbial species of Proteobacteria and
44 Bacteroidetes were significantly and positively correlated with the net nitrification and
45 mineralisation potentials. Our results indicated that microbial subgroups sharing similar niches,
46 instead of total microbial abundances and functional gene abundances, could be important factors
47 affecting the net nitrogen mineralisation potential.

48

49

50 **Keywords**

51 Soil microbial community, co-occurrence network, modules, nitrogen cycle

52

53 **Declarations**54 **Funding**

55 This study was supported by JSPS-KAKENHI: 18H02241, 26292085, 23780166

56

57 **Conflict of interest**

58 The authors declare that they have no conflict of interest.

59

60 **Availability of data and material**

61 The datasets generated during and/or analysed during the current study are available from the
62 corresponding author on reasonable request.

63

64 **Code availability**

65 Not applicable

66

67 **Authors' contribution**

68 MN, SI and RT conceived and designed the experiment; MN, SI and RT performed the experiment;
69 MN, SI, CT and TT performed data analysis; MN prepared figures and tables; MN and RT took the
70 lead in writing the manuscript with input from all authors.

71

72 **Acknowledgements**

73 We would like to thank Dr. Takahito Yoshioka, Dr. Kazuya Kobayashi and the member of Forest
74 Information Laboratory for the helpful suggestion. We also thank Takayuki Yamauchi, Yasuyuki
75 Shibata, Tomoyuki Nakagawa, Jun Yanagimoto, Ken-ichi Ohta, Yuhei Nishioka, Makoto Furuta,
76 Yasunori Kishimoto, Yoichiro Kitagawa, Masaru Okuda, Akira Yamanaka, Yuta Miyagi, Syuichi
77 Sato, Yukie Kawamura and Michiko Shimizu as the staffs of Hokkaido forest research station, Field
78 Science Education and Research Center, Kyoto University for helping the experiments. This study
79 was supported by JSPS-KAKENHI (No. 23780166, 26292085, 18H02241).

80

81

82 **Introduction**

83

84 The availability of nitrogen (N) often limits the primary production of temperate forests (Vitousek
85 and Howarth, 1991; LeBauer and Treseder, 2008). Nitrogen mineralisation and nitrification, wherein
86 organic N is converted into plant-available N forms, are the key processes regulating aboveground
87 and belowground net primary production and N cycling in forest ecosystems (Aber *et al.*, 1985;
88 Reich *et al.*, 1997; Tateno *et al.*, 2004). Soil microbial communities, including fungi and bacteria, are
89 thought to be the main drivers of soil N transformation processes (Schimel and Bennett, 2004; Isobe
90 and Ohte, 2014; Tatsumi *et al.*, 2019; Isobe *et al.*, 2020). Therefore, to understand the forest soil N
91 cycle, it is essential to understand soil microbial communities.

92 In the last two decades, studies have revealed that microbial abundances, communities,
93 and functional gene abundances are affected by environmental conditions including pH,
94 carbon/nitrogen (C/N) ratio, and availability of nutrients and substrates (Högberg *et al.*, 2007;
95 Lauber *et al.*, 2008; Ushio *et al.*, 2010; Wan *et al.*, 2015). Therefore, soil microbial communities can
96 respond to changes in environmental conditions caused by seasons and/or tree species composition
97 of the forests (Moore-Kucera and Dick, 2008; Ushio *et al.*, 2010; Prevost-Boure *et al.*, 2011).
98 Individual tree species also affect soil microbial communities directly by organic carbon supply from
99 their roots (Kaiser *et al.*, 2010, 2011; Urbanová *et al.*, 2015), which can change between seasons
100 and/or with the tree species composition of forests. In particular, mycorrhizal fungi rely on the
101 carbon supply from their symbiotic trees (Gessler *et al.*, 1998; Högberg *et al.*, 2010; Ekblad *et al.*,
102 2013), which can affect the free-living microbial community that is involved in soil N
103 transformation processes (Tatsumi *et al.*, 2020).

104 Furthermore, relationships between microbial communities and soil N transformation
105 processes have been reported in earlier studies (Boyle *et al.*, 2008; Gubry-Rangin *et al.*, 2010; Isobe

106 *et al.*, 2015, 2020; Ribbons *et al.*, 2016; Tatsumi *et al.*, 2020). For example, Ribbons *et al.* (2016)
107 found that the total bacterial abundance had a positive and significant correlation with N
108 mineralisation rates. In addition, rare bacterial and archaeal groups sometimes have significant roles
109 in specific processes (Caffrey *et al.*, 2007; Isobe and Ohte, 2014; Isobe *et al.*, 2020). For example,
110 the abundance of ammonia-oxidising bacteria and archaea (AOB and AOA, respectively) affected
111 the nitrification rate (Isobe *et al.*, 2015, 2020; Ribbons *et al.*, 2016). However, since microbial
112 functions and metabolisms have high diversities (Torsvik and Øvreås, 2002; Strickland *et al.*, 2009;
113 Mendes *et al.*, 2014; Lladó *et al.*, 2016; Wilhelm *et al.*, 2019), the underlying mechanisms by which
114 microbial communities drive N transformation processes are still largely unknown.

115 Recently, the microbial co-occurrence network analysis has provided new insights for
116 understanding microbial communities (Toju *et al.*, 2016; Sun *et al.*, 2017; Nakayama *et al.*, 2019). It
117 has detected densely co-occurring microbial subgroups, called modules (Newman, 2006; Langfelder
118 and Horvath, 2008; Deng *et al.*, 2012), and the analyses of these modules could be used to uncover
119 ecologically relevant interactions that could not be detected by the traditional analyses of community
120 compositions and abundances. Although it is difficult to detect which co-occurring relationships
121 could be a direct physical interaction or an apparent co-occurrence, the microbial subgroups detected
122 as modules would have an individual preference for substrates and environmental conditions (Deng
123 *et al.*, 2012; de Menezes *et al.*, 2015; Jones and Hallin, 2019). Highlighting the microbial modular
124 subgroups would allow for a detailed investigation of the microbial communities that could not be
125 achieved by analysing the whole microbial community (de Menezes *et al.*, 2015). For example,
126 Purahong *et al.* (2016) reported that individual fungal sub-communities detected as modules had
127 different preferences for the chemical compositions of leaf litter, and only a part of the detected
128 modules had significant roles in litter degradation. Thus, investigating the relationships between
129 modular microbial subgroups and N mineralisation processes would reveal the detailed mechanisms

130 of microbial regulation for soil N transformation.

131 Recently, we investigated the impact of conversion of a forest to a monoculture plantation
132 on the characteristics of microbial communities, such as the diversities and co-occurrence network
133 structures of the communities. We found that forest conversion reduced the robustness of the
134 co-occurrence network in mineral soil, while microbial diversities were maintained (Nakayama *et al.*,
135 2019). We also reported that chemical properties, including pH and the C/N ratio, significantly
136 varied among seasons but not among forest types (Nakayama *et al.*, 2019). However, the details of
137 the interactions between each functional group of the microbial communities and the N
138 mineralisation processes are still unknown. Therefore, in the current study, we aimed to reveal the
139 relationships between the roles of each group of microbial communities and the N transformation
140 processes in the soil of a cool temperate forest. We measured the net nitrification and N
141 mineralisation potentials, total gene abundances of bacteria, archaea, and fungi, and the bacterial and
142 archaeal *amoA* gene abundances among forest types (monoculture larch and fir plantations, and
143 natural deciduous broad-leaved forests) and months (May, July, August, September, and November).
144 Furthermore, we predicted the bacterial functional gene abundances, fungal guilds, and trophic
145 modes by using the sequencing results reported previously (Nakayama *et al.*, 2019). Moreover, a
146 microbial co-occurrence network was constructed and the microbial community was divided into
147 modules. We then analysed the relationships between the microbial modules and the net N
148 transformation processes. We hypothesised that: (1) microbial abundance and functional
149 communities change due to the differences in seasons and/or forest types, (2) differences in
150 microbial abundance and functional communities regulate changes in the N transformation processes,
151 (3) individual modules in the co-occurrence network each have relationships with N mineralisation
152 and nitrification potentials, and (4) modules that fluctuate with differences in seasons and forest
153 types are particularly important for the N mineralisation and nitrification potentials.

154

155 **Materials and Methods**

156

157 *Study site and soil sampling*

158

159 We conducted this study in cool-temperate deciduous broad-leaved natural forests (hereafter referred
160 to as “Natural”) and two kinds of plantations (“Larch” and “Fir”) that were converted from natural
161 forests in the Shibeche Branch of the Hokkaido Forest Research Station at the Field Science
162 Education and Research Center, Kyoto University, in north-east Japan (43°24.2’N, 144°38.5’E). The
163 mean annual precipitation and air temperature were 1,189 mm and 6.3°C (1986–2015), respectively.
164 The highest average air and soil temperatures were usually observed in August, while leaves fell
165 from deciduous trees in October (Nakayama and Tateno, 2018). The soils at this site were
166 characterised as andosols (IUSS Working Group WRB, 2015).

167 Natural forests were typically dominated by *Quercus crispula* Blume, *Ulmus davidiana* var.
168 *japonica* Nakai, *Phellodendron amurense* Rupr., *Acer pictum* Thunb. subsp. *mono* (Maxim.) H.
169 Ohashi, and *Fraxinus mandshurica* Rupr. var. *japonica*, and the forest floor was densely covered
170 with *Sasa nipponica* Makino et Shibata. The Larch and Fir plantations were plantations of *Larix*
171 *kaempferi* (Lamb.) Carr. and *Abies sachalinensis* (Shmidt) Masters, respectively. We established four
172 plots in each of the three forest types (Natural, Larch, and Fir) for soil sampling. The dominant trees
173 of all the forest types were ectomycorrhizal trees (Matsuoka *et al.*, 2020). On May 29, July 15,
174 August 26, September 17, and November 9, 2012, five surface mineral soil cores (0–10 cm depth)
175 were collected using a cylindrical soil core sampler (20 cm² in surface area) from each plot and
176 composited. The details of sampling plots and soil sampling have been reported previously
177 (Nakayama *et al.*, 2019).

178 The samples were sieved with a 4 mm mesh sieve and divided into subsamples for wet,
179 fumigation, oven dry, and frozen treatments. The chemical properties (pH, moisture content,
180 microbial biomass C and N, total C and N, and the concentrations of dissolved organic C, NO₃⁻-N,
181 NH₄⁺-N, dissolved inorganic N, amino acid, and dissolved organic N) of the wet and oven-dry
182 samples were previously reported (Nakayama *et al.*, 2019) and summarised in Supplementary Table
183 1. Briefly, the investigated chemical properties except for the C/N ratio significantly differed
184 between sampling months. For example, average pH ranged from 4.5 to 5.6 and was significantly
185 lower in August (Supplementary Table 1; means ± standard deviations; 4.5 ± 0.2, 4.8 ± 0.2, and 4.5 ±
186 0.4 for Larch, Fir, and Natural, respectively). There were no significant differences in other chemical
187 properties except for the microbial biomass of C and N among the forest types, which were
188 significantly higher in Natural than Fir (Supplementary Table 1).

189 DNA was also extracted from frozen subsamples (stored at -20°C) using a DNA extraction
190 kit (DNeasy Power Soil Kit, QIAGEN, Hilden, Germany), sequenced by the Ion Personal Genome
191 Machine™ (PGM™) with the Ion 318™ Chip V2 (Thermo Fisher Scientific, Waltham, MA, USA)
192 and the sequence data were processed. Detailed methods and results of the chemical properties, DNA
193 extraction and sequencing are shown in a previous report (Nakayama *et al.*, 2019), and the sequence
194 data were deposited in the DDBJ Sequence Read Archive under accession number DRA007965.

195

196 *Net nitrification and mineralisation potentials*

197

198 Wet subsamples (30 g) were put in plastic bottles and aerobically incubated for one month at 25°C.
199 To maintain the soil moisture at initial values, ion-exchanged water was added every ten days. After
200 the incubation period, ten grams of each subsample were extracted in 100 ml of 0.5 M K₂SO₄
201 solution. The net nitrification and mineralisation potentials were calculated as the net increase in the

202 amount of NO_3^- -N and the total inorganic N over the incubation period, respectively. The initial
203 values of NH_4^+ -N and NO_3^- -N were reported by Nakayama et al. (2019).

204

205 *Microbial gene quantifications and functional predictions*

206

207 Microbial gene abundance was quantified by the real-time quantitative polymerase chain reaction
208 (qPCR) performed by the LightCycler 96 System (Roche Diagnostics K.K., Mannheim, Germany),
209 with an intercalating dye, SYBR Green I (FastStart Essential DNA Green Master, Roche Diagnostics
210 K.K., Mannheim, Germany). The bacterial and archaeal 16S rRNA genes, fungal ITS regions of the
211 rRNA genes, and the bacterial and archaeal ammonia monooxygenase genes (*amoA*) were quantified
212 to estimate total bacteria, total archaea, total fungi, AOB and AOA, respectively. The bacterial 16S,
213 archaeal 16S, fungal ITS, bacterial *amoA*, and archaeal *amoA* were determined using universal
214 primer sets 338f (Amann *et al.*, 1990)/518r (Muyzer *et al.*, 1993), 109f (Großkopf *et al.*, 1998)/344r
215 (Raskin *et al.*, 1994), ITS1F_KYO2/ITS2_KYO2 (Toju *et al.*, 2012), *amoA* 1F/*amoA* 2R
216 (Rotthauwe *et al.*, 1997), and CrenamoA 23F/CrenamoA 616R (Tourna *et al.*, 2008), respectively.
217 The amplifications of bacterial and archaeal 16S and fungal ITS were performed under the following
218 conditions: an initial denaturation at 95°C for 10 min, followed by 45 cycles at 95°C for 1 min, 53°C
219 for 30 s and 72°C for 1 min (Fierer *et al.*, 2005). The amplification of bacterial and archaeal *amoA*
220 was performed under the following conditions: an initial denaturation at 95°C for 10 min, followed
221 by 45 cycles of 95°C for 1 min, 55°C (for bacterial *amoA*) or 52°C (for archaeal *amoA*) for 30 s, and
222 72°C for 30 s (Okano *et al.*, 2004). More details are described in previous reports (Iwaoka *et al.*,
223 2018; Tatsumi *et al.*, 2019).

224 The bacterial functional genes and the fungal trophic modes and guilds were predicted by
225 using PICRUST pipeline (Langille *et al.*, 2013) and FUNGuild database (Nguyen *et al.*, 2016) based

226 on previously published rarefied data of mineral soil 16S rRNA gene sequences and the fungal
227 taxonomic data of the ITS sequence of the samples (Nakayama *et al.*, 2019), respectively. The
228 number of rarefied sequence reads per sample was 1441 for the 16S rRNA gene and 5817 for the ITS
229 region (Nakayama *et al.*, 2019). This corresponded to 1170 bacterial OTUs (186 ± 18 per sample)
230 and 2288 fungal OTUs (99 ± 26 per sample). The estimated counts of genes by PICRUSt were
231 tagged with the KEGG Orthology (Kanehisa *et al.*, 2016). The occurrence of the genes encoding
232 enzymes for N degradation and mineralisation, chitinase (EC 3.2.1.14), N-acetylglucosaminidase
233 (NAGase, EC3.2.1.52), leucine aminopeptidase (EC 3.4.11.1), arginase (EC 3.5.3.1), and urease (EC
234 3.5.1.5) were predicted from the counts of K01183, K01207, K01255, K01476, and K01428,
235 respectively (Isobe *et al.*, 2018; Tatsumi *et al.*, 2020). The activities and genes abundance of these
236 enzymes are commonly measured to evaluate forest soil N cycling (e.g. Saiya-Cork *et al.*, 2002;
237 Sinsabaugh *et al.*, 2008; Isobe *et al.*, 2018; Tatsumi *et al.*, 2020). Furthermore, to test the enzymatic
238 interactions in the network, the occurrences of genes encoding the enzymes involved in nitrification,
239 ammonia monooxygenase (K10944, K10945, K10946), hydroxylamine dehydrogenase (K10535),
240 and nitrite oxidoreductase (K00370, K00371) were predicted by PICRUSt for each OTU occurring
241 in the network. The fungal trophic modes (e.g. saprotroph, symbiotroph) and the guilds within the
242 symbiotrophic fungi (e.g. ectomycorrhiza, arbuscular mycorrhiza, endophyte, lichenised) were
243 predicted by using the online application FUNGuild (Nguyen *et al.*, 2016). FUNGuild frequently
244 predicts multiple trophic modes for a single OTU, such as Pathotroph-Saprotroph, which we then
245 designated to the “Others” category.

246

247 *The microbial co-occurrence network and module level correlation analysis*

248

249 The soil microbial co-occurrence network was constructed by using the same rarefied soil bacterial

250 and fungal sequencing data as functional prediction (1441 and 5817 reads per sample, respectively)
251 that was previously published in Nakayama *et al.* (2019). Because the numbers of bacterial and
252 fungal sequence reads were not enough to analyse the rare OTUs, we mainly focused on the core and
253 abundant microbial community in the network analysis. Our previous study aimed to reveal the
254 difference in network structures among forest types (Nakayama *et al.*, 2019); however, this study
255 tried to explore the relationships between the modules of the microbial co-occurrence network and N
256 cycling processes. Therefore, we reconstructed the mineral soil co-occurrence network using all of
257 the microbial sequencing data of the mineral soil instead of dividing it by forest types. Before the
258 construction of the network, the abundance data for rarefied soil bacteria and fungi were mixed into
259 one dataset to analyse bacterial-bacterial, fungal-fungal, and bacterial-fungal relationships. In total,
260 there were 12 plots (4 plots for each 3 forest types) and 5 sampling dates ($n = 60$). The network
261 construction and module detection followed our previous paper (Nakayama *et al.*, 2019). Briefly, we
262 removed very rare OTUs occurring in less than 1/3 of samples (i.e. less than 20 samples) before the
263 network construction to avoid the network being too complex, enhancing the determination of the
264 core microbial community (Barberán *et al.*, 2012). After this elimination, 190 and 33 OTUs
265 remained for bacteria and fungi, respectively. Spearman's rank correlations were calculated with all
266 remaining OTU pairs, and p -values were processed based on the false discovery rate. When the
267 correlation coefficient ρ and q -value of the OTU pairs were > 0.6 and < 0.001 , respectively, we
268 considered that there was a significant positive co-occurrence relationship between the OTU pair
269 (Chao *et al.*, 2016). The OTUs that had at least one significant co-occurrence relationship with other
270 OTUs occurred in the network as nodes. The network was visualised using the software package
271 Gephi (ver. 0.9.2) (Bastian *et al.*, 2009). Modules in the microbial co-occurrence network were
272 detected based on the fast greedy modularity optimisation algorithm (Clauset *et al.*, 2004).

273 The relationships between modules and factors (chemical properties, N mineralisation

274 potentials, sampling month, and forest type) were assessed by correlation analysis (Deng *et al.*,
275 2012). Briefly, the relative abundance matrix was divided per module and the relative abundances of
276 each OTU was standardised to mean 0 and variance 1. The module eigenvectors were calculated by
277 singular value decomposition following a previous study (Langfelder and Horvath, 2007). The sign
278 of each module eigenvector was fixed by assigning a positive correlation with the average relative
279 abundances across OTUs within modules (Langfelder and Horvath, 2007). We then analysed the
280 Pearson correlation coefficients between the module eigenvalues and factors as the correlations
281 between modules and factors. Categorical factors (sampling month and forest type) were converted
282 as 0 or 1 dummy vectors before analysis. We chose a significance level of $p < 0.05$. We also tested
283 the relationships between the estimated absolute abundances of modules and factors after
284 multiplying each relative abundance by the total bacterial 16S rRNA and total fungal ITS gene
285 abundance.

286

287 *Statistical analysis*

288

289 We used a two-way split-plot factorial analysis of variance (ANOVA) followed by Tukey's honestly
290 significant difference test to examine the differences in the net nitrification and mineralisation
291 potentials, the total bacterial, archaeal and fungal gene abundance, the bacterial and archaeal *amoA*
292 gene abundance, the predicted bacterial functional gene abundance, and the fungal trophic modes
293 and guilds among forest types (Larch, Fir, and Natural), and sampling months (May, July, August,
294 September, and November). The correlations between microbial gene abundances and chemical
295 properties were assessed using Pearson's correlation analysis. We chose a significance level of $p <$
296 0.05 for all statistical analyses. All statistical analyses were conducted using R software (version
297 3.5.0).

298

299 **Results**

300

301 *Changes in net N transformation potentials*

302

303 Net N mineralisation and nitrification were temporally stable (Fig. 1; two-way ANOVA: $F = 0.69$
304 and $p = 0.607$, and $F = 0.63$ and $p = 0.643$, respectively). Net nitrification did not significantly differ
305 among forest type (Fig. 1a; two-way ANOVA: $F = 4.01$ and $p = 0.057$), while natural forest had
306 significantly higher values of net mineralisation potentials throughout all sampling months (Fig. 1b;
307 two-way ANOVA: $F = 12.98$ and $p < 0.002$). The interaction effects of sampling month and forest
308 type on net nitrification and mineralisation were not significant (Fig. 1; two-way ANOVA: $F = 0.76$
309 and $p = 0.644$, and $F = 1.22$ and $p = 0.317$, respectively).

310

311 *Changes in microbial gene abundance*

312

313 There were significant effects of the sampling month on total bacterial and archaeal 16S rRNA gene
314 abundances (two-way ANOVA: $F = 25.58$ and $p < 0.001$, and $F = 22.41$ and $p < 0.001$, respectively).
315 According to Tukey's honestly significant difference test, bacterial abundance was significantly
316 lower in August, while archaeal abundance was higher in August for all three forest types (Fig. 2a, b).
317 Total fungal ITS gene abundance did not differ significantly among sampling months (Fig. 2c;
318 two-way ANOVA: $F = 1.02$ and $p = 0.409$). The total bacterial, archaeal, and fungal gene
319 abundances were similar among the forest types regardless of sampling months (Fig. 2a, b, c;
320 two-way ANOVA: $F = 1.75$ and $p = 0.228$, $F = 2.80$ and $p = 0.114$, and $F = 0.75$ and $p = 0.500$,
321 respectively).

322 Bacterial and archaeal *amoA* gene abundances differed significantly among sampling
 323 months (two-way ANOVA: $F = 8.84$ and $p < 0.001$, and $F = 15.04$ and $p < 0.001$, respectively).
 324 Archaeal *amoA* gene abundance had a similar trend with archaeal 16S rRNA gene abundance, while
 325 bacterial *amoA* gene abundance had the opposite trend of bacterial 16S rRNA gene abundance, i.e.
 326 the abundances of bacterial and archaeal *amoA* gene were significantly higher in August than in
 327 other months for all the forest types (Fig. 2d, e). Bacterial and archaeal *amoA* genes did not
 328 significantly vary among the forest types (Fig. 2d, e; two-way ANOVA: $F = 0.17$ and $p = 0.844$, and
 329 $F = 1.02$ and $p = 0.400$, respectively).

330 There were some significant positive and negative correlations between total bacterial,
 331 archaeal, and fungal gene abundances and chemical properties such as pH, moisture content, and the
 332 C/N ratio (Supplementary Table 2). Among these relationships, only the pH was positively correlated
 333 with bacterial 16S gene abundance (Supplementary Table 2; $R^2 = 0.08$ and $p < 0.05$). In contrast to
 334 the bacterial abundance, pH was negatively correlated with archaeal and fungal gene abundances
 335 (Supplementary Table 2; $R^2 = 0.31$ and $p < 0.001$, and $R^2 = 0.11$ and $p < 0.01$, respectively). The C/N
 336 ratio had a positive and the strongest relationship with fungal ITS gene abundance (Supplementary
 337 Table 2; $R^2 = 0.35$ and $p < 0.001$). There were no significant relationships between the total
 338 microbial gene abundances and N mineralisation potentials (Supplementary Table 2). Bacterial and
 339 archaeal *amoA* genes were also significantly correlated with chemical properties such as pH and
 340 dissolved organic N content (Supplementary Table 2). Bacterial and archaeal gene abundances were
 341 not correlated with the nitrification and mineralisation potentials (Supplementary Table 2).

342

343 *Changes in bacterial predicted functional gene and fungal trophic modes and guilds*

344

345 Among the predicted functional genes (the genes encoding N degrading and mineralising enzymes:

346 chitinase, NAGase, leucine aminopeptidase, arginase, and urease), there were no significant effects
 347 of forest type (Fig. 3; two-way ANOVA: $F = 0.05$ and $p = 0.949$, $F = 0.54$ and $p = 0.601$, $F = 0.15$
 348 and $p = 0.867$, $F = 0.02$ and $p = 0.985$, and $F = 0.37$ and $p = 0.700$, respectively) and sampling
 349 month, except for urease (Fig. 3; two-way ANOVA: $F = 2.36$ and $p = 0.072$, $F = 0.42$ and $p = 0.795$,
 350 $F = 1.19$ and $p = 0.332$, $F = 1.80$ and $p = 0.150$, and $F = 5.03$ and $p < 0.01$, respectively) on their
 351 relative abundance. The relative abundance of urease in August was significantly higher than that in
 352 May, September, and November (Fig. 3e). The estimated absolute abundances of the predicted
 353 functional genes were temporarily changed, reflecting the changes of bacterial 16S rRNA gene
 354 abundance, and were significantly lower in August than in the other months for all three forest types
 355 (Supplementary Fig. 1).

356 The symbiotrophic fungi (Supplementary Fig. 2; 2.0%–81.1% of total fungi) tended to
 357 have a higher relative abundance throughout all sampling months and forest types than the
 358 saprotrophic fungi (Supplementary Fig. 2; 0.3%–30.5% of total fungi), and most of the
 359 symbiotrophic fungi belonged to the ectomycorrhizal guilds (Supplementary Fig. 3; 61.2%–100% of
 360 symbiotrophic fungi). The relative abundance of the ectomycorrhizal fungi differed significantly
 361 among sampling months (two-way ANOVA: $F = 13.65$ and $p < 0.001$), and the abundance was
 362 significantly higher in August than in the other sampling months (Fig. 4). The relative abundance of
 363 the saprotrophic fungi also differed significantly among sampling months and forest types (two-way
 364 ANOVA: $F = 4.65$, $p < 0.05$ and $F = 3.88$, $p < 0.05$ for months and forest types, respectively), and
 365 the abundance was significantly lower in August ($2.7\% \pm 1.6\%$ of total fungi) than in November
 366 ($9.1\% \pm 9.1\%$ of total fungi) and in Fir ($2.1\% \pm 1.2\%$ of total fungi) than in Larch ($10.8\% \pm 7.4\%$ of
 367 total fungi). The estimated absolute abundances of symbiotrophic and ectomycorrhizal fungi differed
 368 among sampling months (Supplementary Fig. 4; two-way ANOVA: $F = 3.74$ and $p < 0.01$, and $F =$
 369 3.87 and $p < 0.01$, respectively), reflecting the results of the relative abundance of trophic modes and

370 the guild (Supplementary Fig. 2 and 3) rather than the total abundance of fungi (Fig. 2c).

371 The relative abundances of bacterial functional genes had significant correlations with
 372 chemical properties (Supplementary Table 3). In particular, the C/N ratio was positively and strongly
 373 correlated with chitinase, NAGase, leucine aminopeptidase, and arginase, and negatively correlated
 374 with urease (Supplementary Table 3; $R^2 = 0.37$ and $p < 0.001$, $R^2 = 0.32$ and $p < 0.001$, $R^2 = 0.48$ and
 375 $p < 0.001$, $R^2 = 0.43$ and $p < 0.001$, and $R^2 = 0.25$ and $p < 0.001$, respectively). Only weak
 376 correlations were found between fungal groups of higher relative abundances (symbiotrophic,
 377 saprotrophic, and ectomycorrhizal fungi) and chemical properties, such as pH and the C/N ratio
 378 (Supplementary Table 3). The relative abundance of saprotrophic fungi positively correlated with
 379 moisture content (Supplementary Table 3; $R^2 = 0.09$ and $p < 0.05$) and the relative abundance of
 380 ectomycorrhiza negatively correlated with pH (Supplementary Table 3; $R^2 = 0.16$ and $p < 0.01$). The
 381 relative abundances of chitinase, NAGase, leucine aminopeptidase, and arginase were significantly
 382 and negatively correlated with net nitrification potential (Supplementary Table 3; $R^2 = 0.16$ and $p <$
 383 0.01 , $R^2 = 0.29$ and $p < 0.001$, $R^2 = 0.17$ and $p < 0.01$, and $R^2 = 0.14$ and $p < 0.01$, respectively), and
 384 urease had a significant and positive relationship with net nitrification (Supplementary Table 3; $R^2 =$
 385 0.27 and $p < 0.001$). The net mineralisation potential had a significant negative relationship with
 386 NAGase only (Supplementary Table 3; $R^2 = 0.08$ and $p < 0.05$). The relative abundances of the
 387 fungal groups did not have significant relationships with N mineralisation potentials (Supplementary
 388 Table 3).

389 The relationships between the estimated absolute abundances of the bacterial functional
 390 genes and fungi groups, and the net N mineralisation potentials are shown in Supplementary Fig. 5.
 391 The bacterial functional genes, except urease, were significantly and negatively correlated with net
 392 nitrification potentials (Supplementary Fig. 5; $R^2 = 0.10$ and $p < 0.05$ for chitinase, $R^2 = 0.09$ and $p <$
 393 0.05 for NAGase, $R^2 = 0.07$ and $p < 0.05$ for leucine aminopeptidase, and $R^2 = 0.08$ and $p < 0.05$).

394 The estimated absolute abundances of the fungal groups had no significant correlations with net N
395 transformation processes (Supplementary Fig. 5).

396

397 *Modules and microbial functions in the co-occurrence network and their relationships with net N*
398 *transformation potentials*

399

400 The microbial co-occurrence network was divided into 13 modules (Fig. 5a). Modules 1 to 6 had a
401 higher number of OTUs belonging to the modules (12–18 OTUs) and higher relative abundances
402 representing these larger modules, while modules 7 to 13 had only 2 to 4 OTUs and lower relative
403 abundances, except for module 9, which occupied 9.76% of the total fungal community (Fig. 5b, c);
404 further analyses focused on modules 1 to 6. The relatively higher numbers of OTUs within modules
405 2 to 4 belonged to the phylum Acidobacteria (Fig. 5b; 10, 5, and 14 OTUs for each module,
406 respectively), and most of the Acidobacteria belonged to order Acidobacteriales (class
407 Acidobacteria) in module 3, while there were many OTUs belonging to Ellin6513 (class DA052) in
408 modules 2 and 4 (Supplementary Fig. 6 and Supplementary Table 4). Modules 5 and 6 had 8 and 10
409 OTUs belonging to the phylum Proteobacteria, respectively (Fig. 5b). Module 1 tended to have
410 many OTUs of the Proteobacteria and Bacteroidetes (Fig. 5b and Supplementary Fig. 4).

411 The OTUs that were predicted to have the genes responsible for N degradation enzymes
412 (chitinase, NAGase, leucine aminopeptidase, arginase, and urease) and for nitrification enzymes
413 (ammonia oxidation, hydroxylamine oxidation, and nitrite oxidation) investigated in this study were
414 depicted in the co-occurrence network, as shown in Figs. 6 and 7, respectively. Most of the OTUs in
415 the microbial co-occurrence network were predicted to have genes encoding NAGase and leucine
416 aminopeptidase regardless of the modules, while the numbers of OTUs having other functional
417 genes differed among modules (Fig. 6). The OTUs belonging to modules 2, 3, and 4 tended to have

418 the gene encoding chitinase, while relatively lower rates of the OTUs belonging to modules 5 and 6
 419 were predicted to have that gene (Fig. 6a). In contrast, many OTUs belonging to modules 5 and 6
 420 were predicted to have the gene responsible for urease, while modules 2, 3, and 4 had no or very few
 421 OTUs predicted to have the gene (Fig. 6d). There was no OTU that was predicted to have the genes
 422 responsible for ammonia monooxygenase, which is involved in the step from ammonia to
 423 hydroxylamine (K10944, K10945, and K10946) in the co-occurrence network (Fig. 7a). Some links
 424 between the OTUs that were predicted to have the gene responsible for hydroxylamine oxidation
 425 (K10535), and the OTUs that were predicted to have at least one gene responsible for nitrite
 426 oxidation (K00370, K00371) could be detected in module 6 and partly in module 5 (Fig. 7b, c). The
 427 genes for denitrification were also depicted in the co-occurrence network (Supplementary Fig. 7).
 428 There was only one link in module 1 between the first two steps, while some links were found in
 429 modules 4, 5, and 6 for nitric oxide production and consumption, and in modules 2 and 4 for the
 430 nitrous oxide production and consumption (Supplementary Fig. 7).

431 The sampling month did not significantly affect the relative abundances of modules 1 to 6
 432 (Supplementary Fig. 8). The relative abundances of modules 1 to 3 and 6 had significant positive or
 433 negative correlations with forest types; for example, module 1 had a significantly higher relative
 434 abundance in the natural forest, while it was significantly lower in the fir forest (Supplementary Fig.
 435 8; $R^2 = 0.32$ and $p < 0.001$, and $R^2 = 0.20$ and $p < 0.001$, respectively). There was no significant
 436 relationship between modules 4 and 5, and forest types (Supplementary Fig. 8). The net nitrification
 437 potential had significant positive correlations with the relative abundances of modules 1 and 5, and
 438 negative correlations with modules 2 and 4 (Fig. 8a; $R^2 = 0.40$ and $p < 0.001$, $R^2 = 0.10$ and $p < 0.05$,
 439 $R^2 = 0.07$ and $p < 0.05$, and $R^2 = 0.18$ and $p < 0.001$, respectively). On the contrary, the net
 440 mineralisation potential only had a significant positive correlation with module 1 (Fig. 8a; $R^2 = 0.16$
 441 and $p < 0.01$). The chemical properties were also significantly and positively or negatively correlated

442 with individual modules, particularly pH, moisture content and the C/N ratio were significantly
443 correlated with the relative abundances of the modules (Supplementary Fig. 9).

444 The estimated absolute abundances of modules 1 to 6, calculated by multiplying the total
445 bacterial 16S rRNA and fungal ITS genes, were significantly and negatively correlated with the
446 month of August (Supplementary Fig. 10; from module 1 to 6, $R^2 = 0.17$ and $p < 0.01$, $R^2 = 0.16$ and
447 $p < 0.01$, $R^2 = 0.13$ and $p < 0.01$, $R^2 = 0.16$ and $p < 0.01$, $R^2 = 0.10$ and $p < 0.05$, and $R^2 = 0.18$ and $p <$
448 0.001 , respectively), which reflected the temporal changes of the total bacterial 16S rRNA gene
449 abundance (Fig. 2a). There were no significant correlations between the estimated absolute
450 abundances of the modules and the other sampling months (Supplementary Fig. 10). The effects of
451 forest types on the estimated absolute abundances of modules 1 to 6 showed similar trends with the
452 relative abundances, e.g. the estimated absolute abundance of module 1 was higher in the natural
453 forest and lower in the fir forest (Supplementary Fig. 10; $R^2 = 0.15$ and $p < 0.01$, and $R^2 = 0.16$ and p
454 < 0.01 , respectively). The net nitrification potential had a significant positive correlation with the
455 estimated absolute abundance of module 1 and a negative correlation with module 4 (Fig. 8b; $R^2 =$
456 0.20 and $p < 0.001$, and $R^2 = 0.16$ and $p < 0.01$, respectively). There was no significant relationship
457 between the estimated absolute abundances of modules 1 to 6 and the net mineralisation potential
458 (Fig. 8b).

459

460 **Discussion**

461

462 *Differences in microbial communities and N transformation among seasons and forest types*

463

464 We hypothesised that microbial abundance and functional communities changed due to the
465 differences in seasons and/or forest types (hypothesis 1). Regarding this hypothesis, the effect of
466 season on microbial abundance and functional communities was more significant than the effect of
467 forest type (Figs. 2 and 4). However, the effect of season differed between bacteria and fungi, i.e.
468 seasonal differences were apparent for the total abundance of bacteria and for the functional
469 compositions of the fungi (Figs. 2 and 4). In the mid-summer, trees allocate more of their newly
470 synthesised carbon to ectomycorrhizal fungi (EMF) (Högberg *et al.*, 2010) in order to take up more
471 nutrients (Gessler *et al.*, 1998). The seasonal differences of carbon allocation from trees to EMF
472 would explain the higher relative abundance of ectomycorrhizal guilds in mid-summer. In contrast,
473 the abundance of saprotrophic fungi was suppressed in the mid-summer. Saprotrophic fungi decrease
474 in abundance with increasing aridity (Tatsumi *et al.*, 2019). This suggests that the lower soil
475 moisture content in the mid-summer (Supplementary Table 1) could lead to the lower relative
476 abundance of saprotrophic fungi. Another explanation of a lower relative abundance of saprotrophic
477 fungi was the suppression by the EMF. Ectomycorrhizal fungi have been reported to compete for
478 resources with saprotrophic fungi (Lindahl *et al.*, 2002; Bödeker *et al.*, 2016). EMF are also strong
479 competitors for nutrients with free-living microbes, including bacteria (Averill *et al.*, 2014; Tatsumi
480 *et al.*, 2020). Furthermore, EMF have the ability to produce antibacterial material that could suppress
481 bacterial species (Assigbetse *et al.*, 2005; Brooks *et al.*, 2011; Shirakawa *et al.*, 2019). Thus, the total
482 bacterial abundance was probably suppressed in mid-summer due to the increase in EMF (Fig. 2).
483 Another possible explanation for the seasonality of bacterial abundances was the seasonal changes in

484 environmental conditions. Among the chemical properties, only the pH significantly and positively
485 affected bacterial gene abundance (Supplementary Table 2). This was consistent with previous
486 findings (Rousk *et al.*, 2009, 2010). Thus, the lower pH in the mid-summer also might affect the
487 bacterial abundance. Osburn *et al.* (2018) found that similar seasonal trends of bacterial and fungal
488 abundances and reported that soil drying in summer decreased the bacterial abundance, while fungal
489 abundance was maintained potentially by the stimulation of mycorrhizal growth by carbon supply
490 from tree roots. In the present study, we could not find such interactions based on the correlational
491 analysis using all data; however, there was still the possibility that the soil moisture content
492 regulated the balance of soil microbial abundance. Although the environmental preferences differ
493 among bacterial species (Supplementary Fig. 9), the soil environmental condition might strongly
494 affect the total bacterial abundance and functional gene abundances.

495 The abundances of the fungal functional groups, particularly the saprotrophic fungi, varied
496 among forest types (Supplementary Fig. 2). The saprotrophic fungi are the main decomposers of
497 recalcitrant organic matter and obtain their energy and carbon sources from litter decomposition
498 (Osono, 2007; Uroz *et al.*, 2016). In general, the evergreen litter (Fir) decomposed slower than the
499 deciduous litters (Larch and Natural), partly because of the accumulation of recalcitrant organic
500 matter in the fir litter (Cornwell *et al.*, 2008). This difference of decomposability would affect the
501 energy acquisition of the saprotrophic fungi. Therefore, the EMF would be still active in the fir
502 forest due to the carbon supply from symbiotic trees, while the saprotrophic fungi might be
503 suppressed by the substrate recalcitrance.

504 Significant differences in the bacterial community structures among seasons and forest
505 types were observed (Nakayama *et al.*, 2019). Surprisingly, the relative abundances of the bacterial
506 functional genes concerning the N mineralisation process were stable across seasons and forest types
507 (Fig. 3). One explanation for this is the functional redundancy of the bacterial community

508 (Nannipieri *et al.*, 2003; Wertz *et al.*, 2006). Frossard *et al.* (2012) reported that there were no
509 relationships between bacterial community structures and potential enzymatic activities because of
510 bacterial functional redundancy. Thus, even if the microbial community structures changed among
511 forest types, the potential to produce extracellular enzymes by the microbes would be maintained in
512 these sites. Another explanation is the methodological limitations of PICRUSt, such as shortage of
513 referenced reference database and restricted OTUs generation method (Douglas *et al.*, 2020).
514 Although PICRUSt has been widely used in the study of soil bacterial functional community (e.g.,
515 Isobe *et al.*, 2018), other methods such as shotgun metagenomic sequencing should be considered for
516 more detailed functional community analysis.

517 The N mineralisation potentials had no consistent relationships with total microbial
518 abundances and functional groups among seasons as well as forest types. Thus, our second
519 hypothesis that the differences in microbial abundance and functional communities regulated the
520 changes of N transformation did not hold. In contrast to the microbial communities not varying
521 among forest types, N mineralisation potentials varied among forest types (Fig. 1). There were three
522 possible explanations for this result. First, litter quality may exert a stronger control on N
523 mineralisation than the microbial factors. Based on the mycorrhizal associated nutrient economy
524 theory (Phillips *et al.*, 2013), the EMF-dominated forest stands, such as the plots in this study tend to
525 have “organic nutrient economy” characterized by slow litter decomposition, and the organic N
526 turnover regulates N availability in the soil (Phillips *et al.*, 2013). As we discussed above, deciduous
527 tree has higher decomposition rate than evergreen. In general, conifer leaves (Larch and Fir) also
528 tend to have a slower decomposition rate than broad leaves (Natural) (Singh and Gupta, 1977).
529 Accordingly, the N transformations might be faster in Natural than Larch and Fir, regardless of
530 microbial dynamics. Second, we measured net N mineralisation and the functional attributes we
531 characterized are more specifically focused on N acquiring enzymes. However, microbial

532 communities also consume mineralised N. While microbial N consumption was not measured and
533 not known in this study, Urakawa *et al.* (2016) reported that the net rates of N mineralisation
534 correlated with its gross rates, respectively, by investigating the net and gross rates of the N
535 transformation processes in 38 forest sites across the Japan archipelago including the sites of this
536 study. Further, some previous studies have reported significant relationships between microbial
537 properties and the net N mineralisation rate (Fraterrigo *et al.*, 2006; Kang *et al.*, 2018). However,
538 there is still the possibility that microbial N consumption masks the relationships between microbes
539 and N transformations, and future research using the gross measurement of N mineralisation is
540 needed to test this. The third possible explanation was that a part of microbial dynamics was
541 important for N mineralisation potentials rather than whole microbial and functional gene abundance.
542 Most bacterial species are considered to relate to N mineralisation (Bottomley *et al.*, 2012; Isobe and
543 Ohte, 2014). Furthermore, strong correlations between enzymatic activities and microbial functional
544 predictions have been reported (Trivedi *et al.*, 2016). However, microbial activity varies widely
545 among species (Fierer *et al.*, 2007; Pinnell *et al.*, 2014; Wilhelm *et al.*, 2019). Thus, as we discuss
546 below for our third and fourth hypotheses, there is the possibility that a subsection of the microbial
547 communities is more active and important for N mineralisation.

548 In terms of the nitrification process, positive relationships between ammonia-oxidising
549 communities and nitrification have been previously reported (Hawkes *et al.*, 2005; Jia and Conrad,
550 2009; Isobe *et al.*, 2015). However, we could not find any significant relationships between them
551 (Supplementary Table 2). Although the ammonia-oxidising prokaryotes markedly increased in
552 mid-summer, the nitrification potential was stable across the seasons. The activities of the
553 ammonia-oxidising prokaryotes are sensitive to environmental conditions, including pH and
554 temperature (Jung *et al.*, 2011; Yao *et al.*, 2011; Zhang *et al.*, 2012; Taylor *et al.*, 2017). The
555 activities of nitrifying communities might be low in the mid-summer in our study site because of the

556 lower pH, although further research focusing on the gross nitrification is needed as we discussed
557 above. Furthermore, the proportions of the net nitrification and mineralisation potentials suggest that
558 most of the mineralised N underwent the steps of nitrification at this study site (Fig. 1). The
559 mineralisation step might limit the nitrification potentials at the site. There was also another
560 explanation. In this study, we measured bacterial and archaeal *amoA* genes as the microbial factors
561 because the *amoA* genes involved in the ammonia-oxidation, the first and rate-limiting step of
562 nitrification (Isobe et al., 2011). Indeed, Isobe et al. (2018) reported that gross nitrification rate and
563 soil NO_3^- concentration related to the AOB population in the natural forest of this study site.
564 However, some bacteria completely oxidize ammonium into nitrate, which is called comammox, and
565 has different enzymes from AOB (Costa et al., 2006). Comammox could be the main driver of
566 nitrification in some ecosystems (Osburn and Barrett, 2020). A part of fungal groups also involved in
567 the nitrification processes (Zhu et al., 2015). Thus, those other nitrifying communities that we did
568 not measure might drive the nitrification process.

569

570 *Modules in the microbial co-occurrence network*

571

572 Our results showed that each module was differently related to N transformation processes at the site.
573 Namely, modules 1 and 5 had significant positive relationships with N transformation processes and
574 modules 2 and 4 had significant negative relationships (Fig. 8). These results affirmed our third
575 hypothesis that individual modules in the co-occurrence network each had relationships with N
576 mineralisation and nitrification potentials.

577 Bacterial species belonging to the Proteobacteria and Bacteroidetes, the main members of
578 modules 1 and 5 (Fig. 5b), tend to have higher abundances in nutrient rich conditions (Fierer *et al.*,
579 2012; Peiffer *et al.*, 2013), implying their copiotrophic strategy. Copiotrophs are reported to have

580 high population turnover and short mean generation time (Fierer *et al.*, 2007). The microbial
581 necromass is a significant source of dissolved organic matter and is recycled and mineralised by
582 microbes (Miltner *et al.*, 2012; Huygens *et al.*, 2016). Hence, *r*-selected bacterial species could lead
583 to more active mineralisation. However, module 6, which consisted mainly of Proteobacteria, did not
584 correlate with net mineralisation potentials (Figs. 5 and 8). The phylum Proteobacteria is the largest
585 bacterial phylum and contains diverse OTUs with diverse functions and metabolisms; even within
586 the same class, their metabolisms vary (Kersters *et al.*, 2006). Therefore, our results indicate that
587 modules 1 and 5 might include OTUs responsible for creating the variation of mineralisation
588 potential, while there might be less important Proteobacteria within module 6. Future research
589 highlighting the members within modules 1 and 5 can reveal the detailed relationships between
590 microbial subgroups and the N transformation processes.

591 In contrast, modules 2 and 4, consisting mainly of the OTUs from the order Ellin6513
592 (Acidobacterial subdivision 2), significantly and negatively correlated with the net mineralisation
593 potentials (Fig. 6 and Supplementary Table 4). The abundance of module 2 differed among forest
594 types, while there were no clear trends for module 4 (Supplementary Figs. 8 and 10). Some of the
595 members of the Acidobacteria adapt to oligotrophic conditions, having the *K*-selected strategy
596 (Fierer *et al.*, 2007; Kielak *et al.*, 2016). Oligotrophic and *K*-selected bacteria have low growth rates,
597 slow population turnover rates and long generation times (Fierer *et al.*, 2007). Therefore, modules 2
598 and 4 might have lower mineralisation potentials than the other modules. Further, modules 2 and 4
599 tended to have higher relative abundances within lower pH conditions (Supplementary Fig. 9).
600 Previous studies have reported that the relative abundance of Acidobacteria, including subdivision 2,
601 was negatively correlated with pH, while other bacterial phyla tended to correlate positively with pH
602 (Lauber *et al.*, 2009; Rousk *et al.*, 2010). In the lower pH environments that the microbes from
603 modules 2 and 4 were abundant in, other bacteria, including the Proteobacteria, would have been

604 suppressed.

605 The possibility that the litter quality rather than microbial community determined the N
606 transformation processes discussed above still could not be rejected. However, the microbial
607 subgroups would be important for the net N transformation processes at the site. We expected that
608 the modules that fluctuated with differences in seasons and forest types were particularly important
609 for the N mineralisation and nitrification potentials in our fourth hypothesis. Indeed, module 1,
610 which had the strongest positive correlations with net N mineralisation and nitrification, varied
611 among the forest types (Supplementary Fig. 8). However, module 5, which also had significant and
612 positive relationships with net nitrification, did not vary among forest types (Supplementary Fig. 8).

613 Further, the relative abundances of analysed microbial modules did not fluctuate seasonally.
614 This was consistent with bacterial community structures and functions (Fig. 3). These results of
615 seasonally stable relative abundances of modules imply that at least core microbial species, which
616 would be important for N transformations, had similar seasonal trends of growth and death.
617 Therefore, our fourth hypothesis was partly affirmed but largely did not hold.

618 The co-occurrence network was constructed mathematically based only on the relative
619 abundance data (Deng *et al.*, 2012). Therefore, it was difficult to separate whether the co-occurring
620 links between two microbial species were actual interactions, such as substrate giving-receiving, or
621 environmental filtering (e.g. niche preferences). In this study, there were only a few links of
622 predicted enzymatic production within the modules in the co-occurrence network (Fig. 7 and
623 Supplementary Fig. 7). Furthermore, individual modules had individual correlations with
624 environmental factors (Supplementary Fig. 9), as shown in previous studies (Deng *et al.*, 2012; de
625 Menezes *et al.*, 2015; Purahong *et al.*, 2016). Thus, the modules of the microbial co-occurrence
626 networks may represent the niche separations of the microbial communities rather than interactions
627 and physical links. Therefore, our results indicate that the niches of microbial sub-communities are

628 the factors important for N mineralisation processes.

629

630 *Conclusions*

631

632 In this study, the results showed that the abundances of microbial communities differed among
633 seasons. However, these seasonal fluctuations of microbial abundances were not related to the net N
634 mineralisation potentials. Instead, the importance of microbial modular sub-groups that shared
635 similar niches for the net N transformation potentials was revealed by the analysis of the
636 co-occurrence network and functional predictions. In this study, because low sequencing reads were
637 obtained and prevented us from analysing rare microbial communities, we focused on the core soil
638 microbial community in the network analysis. Since the network analysis is based on the correlation
639 of (relative) abundance, the difference in total sequence read numbers is not a major problem.
640 Therefore, in future research, the combination of 16S rRNA, amoA, and other functional genes with
641 the network analysis also could be adapted to analyse rare microbes with the core microbial
642 communities as used in this study for bacterial-fungal relationships. Although further research
643 investigating the detailed ecology and functions of the detected microbial subgroups is needed, our
644 findings and approaches provide a key for revealing N cycling by microbial communities in forest
645 soil.

646

647 References

648

 649 Aber, J.D., Melillo, J.M., Nadelhoffer, K.J., McLaugherty, C.A., and Pastor, J. (1985) Fine root turnover
 650 in forest ecosystems in relation to quantity and form of nitrogen availability: a comparison of two
 651 methods. *Oecologia* **66**: 317–321.

652 Amann, R.I., Binder, B.J., Olson, R.J., Chisholm, S.W., Devereux, R., and Stahl, D.A. (1990)

 653 Combination of 16S rRNA-targeted oligonucleotide probes with flow cytometry for analyzing
 654 mixed microbial populations. *Appl Environ Microbiol* **56**: 1919–25.

 655 Assigbetse, K., Gueye, M., Thioulouse, J., and Duponnois, R. (2005) Soil Bacterial Diversity Responses
 656 to Root Colonization by an Ectomycorrhizal Fungus are not Root-Growth-Dependent. *Microb Ecol*
 657 **50**: 350–359.

 658 Averill, C., Turner, B.L., and Finzi, A.C. (2014) Mycorrhiza-mediated competition between plants and
 659 decomposers drives soil carbon storage. *Nature* **505**: 543–545.

 660 Barberán, A., Bates, S.T., Casamayor, E.O., and Fierer, N. (2012) Using network analysis to explore
 661 co-occurrence patterns in soil microbial communities. *ISME J* **6**: 343–351.

 662 Bastian, M., Heymann, S., and Jacomy, M. (2009) Gephi: An Open Source Software for Exploring and
 663 Manipulating Networks. In, *Proceedings of the Third International ICWSM Conference.*, pp.
 664 361–362.

 665 Bödeker, I.T.M., Lindahl, B.D., Olson, Å., and Clemmensen, K.E. (2016) Mycorrhizal and saprotrophic
 666 fungal guilds compete for the same organic substrates but affect decomposition differently. *Funct*
 667 *Ecol* **30**: 1967–1978.

 668 Bottomley, P.J., Taylor, A.E., and Myrold, D.D. (2012) A consideration of the relative contributions of
 669 different microbial subpopulations to the soil N cycle. *Front Microbiol* **3**: 373.

 670 Boyle, S.A., Yarwood, R.R., Bottomley, P.J., and Myrold, D.D. (2008) Bacterial and fungal contributions
 671 to soil nitrogen cycling under Douglas fir and red alder at two sites in Oregon. *Soil Biol Biochem*
 672 **40**: 443–451.

 673 Brooks, D.D., Chan, R., Starks, E.R., Grayston, S.J., and Jones, M.D. (2011) Ectomycorrhizal hyphae
 674 structure components of the soil bacterial community for decreased phosphatase production. *FEMS*
 675 *Microbiol Ecol* **76**: 245–255.

 676 Caffrey, J.M., Bano, N., Kalanetra, K., and Hollibaugh, J.T. (2007) Ammonia oxidation and
 677 ammonia-oxidizing bacteria and archaea from estuaries with differing histories of hypoxia. *ISME J*
 678 **1**: 660–662.

 679 Chao, Y., Liu, W., Chen, Y., Chen, W., Zhao, L., Ding, Q., et al. (2016) Structure, Variation, and
 680 Co-occurrence of Soil Microbial Communities in Abandoned Sites of a Rare Earth Elements Mine.
 681 *Environ Sci Technol* **50**: 11481–11490.

- 682 Clauset, A., Newman, M.E.J., and Moore, C. (2004) Finding community structure in very large networks.
683 *Phys Rev* **70**: 066111.
- 684 Cornwell, W.K., Cornelissen, J.H.C., Amatangelo, K., Dorrepaal, E., Eviner, V.T., Godoy, O., et al.
685 (2008) Plant species traits are the predominant control on litter decomposition rates within biomes
686 worldwide. *Ecol Lett* **11**: 1065–1071.
- 687 Costa, E., Pérez, J., and Kreft, J.U. (2006) Why is metabolic labour divided in nitrification? *Trends*
688 *Microbiol* **14**: 213–219.
- 689 Deng, Y., Jiang, Y.H., Yang, Y., He, Z., Luo, F., and Zhou, J. (2012) Molecular ecological network
690 analyses. *BMC Bioinformatics* **13**: 113.
- 691 Douglas, G.M., Maffei, V.J., Zaneveld, J.R., Yurgel, S.N., Brown, J.R., Taylor, C.M., et al. (2020)
692 PICRUSt2 for prediction of metagenome functions. *Nat Biotechnol* **38**: 685–688.
- 693 Ekblad, A., Wallander, H., Godbold, D.L., Cruz, C., Johnson, D., Baldrian, P., et al. (2013) The
694 production and turnover of extramatrical mycelium of ectomycorrhizal fungi in forest soils: role in
695 carbon cycling. *Plant Soil* **366**: 1–27.
- 696 Fierer, N., Bradford, M.A., and Jackson, R.B. (2007) Toward an ecological classification of soil bacteria.
697 *Ecology* **88**: 1354–1364.
- 698 Fierer, N., Jackson, J.A., Vilgalys, R., and Jackson, R.B. (2005) Assessment of soil microbial community
699 structure by use of taxon-specific quantitative PCR assays. *Appl Environ Microbiol* **71**: 4117–20.
- 700 Fierer, N., Lauber, C.L., Ramirez, K.S., Zaneveld, J., Bradford, M.A., and Knight, R. (2012) Comparative
701 metagenomic, phylogenetic and physiological analyses of soil microbial communities across
702 nitrogen gradients. *ISME J* **6**: 1007–1017.
- 703 Fraterrigo, J.M., Balsler, T.C., and Turner, M.G. (2006) Microbial community variation and its
704 relationship with nitrogen mineralization in historically altered forests. *Ecology* **87**: 570–579.
- 705 Frossard, A., Gerull, L., Mutz, M., and Gessner, M.O. (2012) Disconnect of microbial structure and
706 function: Enzyme activities and bacterial communities in nascent stream corridors. *ISME J* **6**:
707 680–691.
- 708 Gessler, A., Schneider, S., Von Sengbusch, D., Weber, P., Hanemann, U., Huber, C., et al. (1998) Field
709 and laboratory experiments on net uptake of nitrate and ammonium the roots of spruce (*Picea abies*)
710 and beech (*Fagus sylvatica*) trees. *New Phytol* **138**: 275–285.
- 711 Großkopf, R., Janssen, P.H., and Liesack, W. (1998) Diversity and structure of the methanogenic
712 community in anoxic rice paddy soil microcosms as examined by cultivation and direct 16S rRNA
713 gene sequence retrieval. *Appl Environ Microbiol* **64**: 960–969.
- 714 Gubry-Rangin, C., Nicol, G.W., and Prosser, J.I. (2010) Archaea rather than bacteria control nitrification
715 in two agricultural acidic soils. *FEMS Microbiol Ecol* **74**: 566–574.
- 716 Hawkes, C. V., Wren, I.F., Herman, D.J., and Firestone, M.K. (2005) Plant invasion alters nitrogen
717 cycling by modifying the soil nitrifying community. *Ecol Lett* **8**: 976–985.

- 718 Högberg, M.N., Briones, M.J.I., Keel, S.G., Metcalfe, D.B., Campbell, C., Midwood, A.J., et al. (2010)
 719 Quantification of effects of season and nitrogen supply on tree below-ground carbon transfer to
 720 ectomycorrhizal fungi and other soil organisms in a boreal pine forest. *New Phytol* **187**: 485–493.
- 721 Högberg, M.N., Högberg, P., and Myrold, D.D. (2007) Is microbial community composition in boreal
 722 forest soils determined by pH, C-to-N ratio, the trees, or all three? *Oecologia* **150**: 590–601.
- 723 Huygens, D., Díaz, S., Urcelay, C., and Boeckx, P. (2016) Microbial recycling of dissolved organic
 724 matter confines plant nitrogen uptake to inorganic forms in a semi-arid ecosystem. *Soil Biol*
 725 *Biochem* **101**: 142–151.
- 726 Isobe, K., Ise, Y., Kato, H., Oda, T., Vincenot, C.E., Koba, K., et al. (2020) Consequences of microbial
 727 diversity in forest nitrogen cycling: diverse ammonifiers and specialized ammonia oxidizers. *ISME*
 728 *J* **14**: 12–25.
- 729 Isobe, K., Koba, K., Otsuka, S., and Senoo, K. (2011) Nitrification and nitrifying microbial communities
 730 in forest soils. *J For Res* **16**: 351–362.
- 731 Isobe, K. and Ohte, N. (2014) Ecological perspectives on microbes involved in N-cycling. *Microbes*
 732 *Environ* **29**: 4–16.
- 733 Isobe, K., Ohte, N., Oda, T., Murabayashi, S., Wei, W., Senoo, K., et al. (2015) Microbial regulation of
 734 nitrogen dynamics along the hillslope of a natural forest. *Front Environ Sci* **2**: 63.
- 735 Isobe, K., Oka, H., Watanabe, T., Tateno, R., Urakawa, R., Liang, C., et al. (2018) High soil microbial
 736 activity in the winter season enhances nitrogen cycling in a cool-temperate deciduous forest. *Soil*
 737 *Biol Biochem* **124**: 90–100.
- 738 IUSS Working Group WRB (2015) International soil classification system for naming soils and creating
 739 legends for soil maps. World Reference Base for Soil Resources 2014, update 2015.
- 740 Iwaoka, C., Imada, S., Taniguchi, T., Du, S., Yamanaka, N., and Tateno, R. (2018) The Impacts of Soil
 741 Fertility and Salinity on Soil Nitrogen Dynamics Mediated by the Soil Microbial Community
 742 Beneath the Halophytic Shrub Tamarisk. *Microb Ecol* **75**: 985–996.
- 743 Jia, Z. and Conrad, R. (2009) Bacteria rather than Archaea dominate microbial ammonia oxidation in an
 744 agricultural soil. *Environ Microbiol* **11**: 1658–1671.
- 745 Jones, C.M. and Hallin, S. (2019) Geospatial variation in co-occurrence networks of nitrifying microbial
 746 guilds. *Mol Ecol* **28**: 293–306.
- 747 Jung, J., Yeom, J., Kim, J., Han, J., Lim, H.S., Park, H., et al. (2011) Change in gene abundance in the
 748 nitrogen biogeochemical cycle with temperature and nitrogen addition in Antarctic soils. *Res*
 749 *Microbiol* **162**: 1018–1026.
- 750 Kaiser, C., Fuchslueger, L., Koranda, M., Gorfer, M., Stange, C.F., Kitzler, B., et al. (2011) Plants control
 751 the seasonal dynamics of microbial N cycling in a beech forest soil by belowground C allocation.
 752 *Ecology* **92**: 1036–1051.
- 753 Kaiser, C., Koranda, M., Kitzler, B., Fuchslueger, L., Schnecker, J., Schweiger, P., et al. (2010)

- 754 Belowground carbon allocation by trees drives seasonal patterns of extracellular enzyme activities
755 by altering microbial community composition in a beech forest soil. *New Phytol* **187**: 843–858.
- 756 Kang, H., Gao, H., Yu, W., Yi, Y., Wang, Y., and Ning, M. (2018) Changes in soil microbial community
757 structure and function after afforestation depend on species and age: Case study in a subtropical
758 alluvial island. *Sci Total Environ* **625**: 1423–1432.
- 759 Kanehisa, M., Sato, Y., Kawashima, M., Furumichi, M., and Tanabe, M. (2016) KEGG as a reference
760 resource for gene and protein annotation. *Nucleic Acids Res* **44**: D457–D462.
- 761 Kersters, K., DeVos, P., Gills, M., Swings, J., Vandamme, P., and Stackebrandt, E. (2006) Introduction to
762 the proteobacteria. In, Dworkin, M., Falkow, S., Eosenberg, E., Schleifer, K.-H., and Stackbrandt, E.
763 (eds), *The prokaryotes*. New yo: Springer-Verlag, pp. 3–37.
- 764 Kielak, A.M., Barreto, C.C., Kowalchuk, G.A., van Veen, J.A., and Kuramae, E.E. (2016) The ecology of
765 Acidobacteria: Moving beyond genes and genomes. *Front Microbiol* **7**: 744.
- 766 Langfelder, P. and Horvath, S. (2007) Eigengene networks for studying the relationships between
767 co-expression modules. *BMC Syst Biol* **1**: 54.
- 768 Langfelder, P. and Horvath, S. (2008) WGCNA: an R package for weighted correlation network analysis.
769 *BMC Bioinformatics* **9**: 559.
- 770 Langille, M.G.I., Zaneveld, J., Caporaso, J.G., McDonald, D., Knights, D., Reyes, J.A., et al. (2013)
771 Predictive functional profiling of microbial communities using 16S rRNA marker gene sequences.
772 *Nat Biotechnol* **31**: 814–821.
- 773 Lauber, C.L., Hamady, M., Knight, R., and Fierer, N. (2009) Pyrosequencing-based assessment of soil pH
774 as a predictor of soil bacterial community structure at the continental scale. *Appl Environ Microbiol*
775 **75**: 5111–20.
- 776 Lauber, C.L., Strickland, M.S., Bradford, M.A., and Fierer, N. (2008) The influence of soil properties on
777 the structure of bacterial and fungal communities across land-use types. *Soil Biol Biochem* **40**:
778 2407–2415.
- 779 LeBauer, D.S. and Treseder, K.K. (2008) Nitrogen limitation of net primary productivity in terrestrial
780 ecosystems is globally distributed. *Ecology* **89**: 371–379.
- 781 Lindahl, B.O., Taylor, A.F.S., and Finlay, R.D. (2002) Defining nutritional constraints on carbon cycling
782 in boreal forests-towards a less “phytcentric” perspective. *Plant Soil* **242**: 123-135
- 783 Lladó, S., Žifčáková, L., Větrovský, T., Eichlerová, I., and Baldrian, P. (2016) Functional screening of
784 abundant bacteria from acidic forest soil indicates the metabolic potential of Acidobacteria
785 subdivision 1 for polysaccharide decomposition. *Biol Fertil Soils* **52**: 251–260.
- 786 Matsuoka, S., Sugiyama, Y., Tatenno, R., Imamura, S., Kawaguchi, E., and Osono, T. (2020) Evaluation of
787 host effects on ectomycorrhizal fungal community compositions in a forested landscape in northern
788 Japan. *R Soc Open Sci* **7**: 191952.
- 789 Mendes, L.W., Kuramae, E.E., Navarrete, A.A., Van Veen, J.A., and Tsai, S.M. (2014) Taxonomical and

- 790 functional microbial community selection in soybean rhizosphere. *ISME J* **8**: 1577–1587.
- 791 de Menezes, A.B., Prendergast-Miller, M.T., Richardson, A.E., Toscas, P., Farrell, M., Macdonald, L.M.,
792 et al. (2015) Network analysis reveals that bacteria and fungi form modules that correlate
793 independently with soil parameters. *Environ Microbiol* **17**: 2677–2689.
- 794 Miltner, A., Bombach, P., Schmidt-Brücken, B., and Kästner, M. (2012) SOM genesis: Microbial
795 biomass as a significant source. *Biogeochemistry* **111**: 41–55.
- 796 Moore-Kucera, J. and Dick, R.P. (2008) PLFA profiling of microbial community structure and seasonal
797 shifts in soils of a Douglas-fir chronosequence. *Microb Ecol* **55**: 500–511.
- 798 Muyzer, G., de Waal, E.C., and Uitterlinden, A.G. (1993) Profiling of complex microbial populations by
799 denaturing gradient gel electrophoresis analysis of polymerase chain reaction-amplified genes
800 coding for 16S rRNA. *Appl Environ Microbiol* **59**: 695–700.
- 801 Nakayama, M., Imamura, S., Taniguchi, T., and Tateno, R. (2019) Does conversion from natural forest to
802 plantation affect fungal and bacterial biodiversity, community structure, and co-occurrence
803 networks in the organic horizon and mineral soil? *For Ecol Manage* **446**: 238–250.
- 804 Nakayama, M. and Tateno, R. (2018) Solar radiation strongly influences the quantity of forest tree root
805 exudates. *Trees* **32**: 871–879.
- 806 Nannipieri, P., Ascher, J., Ceccherini, M.T., Landi, L., Pietramellara, G., and Renella, G. (2003)
807 Microbial diversity and soil functions. *Eur J Soil Sci* **54**: 655–670.
- 808 Newman, M.E.J. (2006) Modularity and community structure in networks. *Proc Natl Acad Sci U S A* **103**:
809 8577–8582.
- 810 Nguyen, N.H., Song, Z., Bates, S.T., Branco, S., Tedersoo, L., Menke, J., et al. (2016) FUNGuild: An
811 open annotation tool for parsing fungal community datasets by ecological guild. *Fungal Ecol* **20**:
812 241–248.
- 813 Okano, Y., Hristova, K.R., Leutenegger, C.M., Jackson, L.E., Denison, R.F., Gebreyesus, B., et al. (2004)
814 Application of Real-Time PCR To Study Effects of Ammonium on Population Size of
815 Ammonia-Oxidizing Bacteria in Soil. *Appl Environ Microbiol* **70**: 1008–1016.
- 816 Osburn, E.D. and Barrett, J.E. (2020) Abundance and functional importance of complete
817 ammonia-oxidizing bacteria (comammox) versus canonical nitrifiers in temperate forest soils. *Soil*
818 *Biol Biochem* **145**: 107801.
- 819 Osburn, E.D., Elliott, K.J., Knoepp, J.D., Miniati, C.F., and Barrett, J.E. (2018) Soil microbial response to
820 Rhododendron understory removal in southern Appalachian forests: Effects on extracellular
821 enzymes. *Soil Biol Biochem* **127**: 50–59.
- 822 Osono, T. (2007) Ecology of ligninolytic fungi associated with leaf litter decomposition. *Ecol Res* **22**:
823 955–974.
- 824 Peiffer, J.A., Spor, A., Koren, O., Jin, Z., Tringe, S.G., Dangl, J.L., et al. (2013) Diversity and heritability
825 of the maize rhizosphere microbiome under field conditions. *Proc Natl Acad Sci U S A* **110**:

- 826 6548–6553.
- 827 Phillips, R.P., Brzostek, E., and Midgley, M.G. (2013) The mycorrhizal-associated nutrient economy: A
 828 new framework for predicting carbon-nutrient couplings in temperate forests. *New Phytol* **199**:
 829 41–51.
- 830 Pinnell, L.J., Dunford, E., Ronan, P., Hausner, M., and Neufeld, J.D. (2014) Recovering glycoside
 831 hydrolase genes from active tundra cellulolytic bacteria. *Can J Microbiol* **60**: 469–476.
- 832 Prevost-Boure, N.C., Maron, P.A., Ranjard, L., Nowak, V., Dufrene, E., Damesin, C., et al. (2011)
 833 Seasonal dynamics of the bacterial community in forest soils under different quantities of leaf litter.
 834 *Appl Soil Ecol* **47**: 14–23.
- 835 Purahong, W., Krüger, D., Buscot, F., and Wubet, T. (2016) Correlations between the composition of
 836 modular fungal communities and litter decomposition-associated ecosystem functions. *Fungal Ecol*
 837 **22**: 106–114.
- 838 Raskin, L., Stromley, J.M., Rittmann, B.E., and Stahl, D.A. (1994) Group-specific 16S rRNA
 839 hybridization probes to describe natural communities of methanogens. *Appl Environ Microbiol* **60**:
 840 1232–1240.
- 841 Reich, P.B., Grigal, D.F., Aber, J.D., and Gower, S.T. (1997) Nitrogen mineralization and productivity in
 842 50 hardwood and conifer stands on diverse soils. *Ecology* **78**: 335–347.
- 843 Ribbons, R.R., Levy-Booth, D.J., Masse, J., Grayston, S.J., McDonald, M.A., Vesterdal, L., and Prescott,
 844 C.E. (2016) Linking microbial communities, functional genes and nitrogen-cycling processes in
 845 forest floors under four tree species. *Soil Biol Biochem* **103**: 181–191.
- 846 Rothauwe, J.H., Witzel, K.P., and Liesack, W. (1997) The ammonia monooxygenase structural gene
 847 amoA as a functional marker: molecular fine-scale analysis of natural ammonia-oxidizing
 848 populations. *Appl Environ Microbiol* **63**: 4704–12.
- 849 Rousk, J., Bååth, E., Brookes, P.C., Lauber, C.L., Lozupone, C., Caporaso, J.G., et al. (2010) Soil
 850 bacterial and fungal communities across a pH gradient in an arable soil. *ISME J* **4**: 1340–1351.
- 851 Rousk, J., Brookes, P.C., and Bååth, E. (2009) Contrasting soil pH effects on fungal and bacterial growth
 852 suggest functional redundancy in carbon mineralization. *Appl Environ Microbiol* **75**: 1589–96.
- 853 Saiya-Cork, K.R., Sinsabaugh, R.L., and Zak, D.R. (2002) The effects of long term nitrogen deposition
 854 on extracellular enzyme activity in an *Acer saccharum* forest soil. *Soil Biol Biochem* **34**:
 855 1309–1315.
- 856 Schimel, J.P. and Bennett, J. (2004) Nitrogen mineralization: Challenges of a changing paradigm.
 857 *Ecology* **85**: 591–602.
- 858 Shirakawa, M., Uehara, I., and Tanaka, M. (2019) Mycorrhizosphere Bacterial Communities and their
 859 Sensitivity to Antibacterial Activity of Ectomycorrhizal Fungi. *Microbes Environ* **34**: 191–198.
- 860 Singh, J.S. and Gupta, S.R. (1977) Plant decomposition and soil respiration in terrestrial ecosystems. *Bot*
 861 *Rev* **43**: 449–528.

- 862 Sinsabaugh, R.L., Lauber, C.L., Weintraub, M.N., Ahmed, B., Allison, S.D., Crenshaw, C., et al. (2008)
 863 Stoichiometry of soil enzyme activity at global scale. *Ecol Lett* **11**: 1252–1264.
- 864 Strickland, M.S., Lauber, C., Fierer, N., and Bradford, M.A. (2009) Testing the functional significance of
 865 microbial community composition. *Ecology* **90**: 441–451.
- 866 Sun, S., Li, S., Avera, B.N., Strahm, B.D., and Badgley, B.D. (2017) Soil bacterial and fungal
 867 communities show distinct recovery patterns during forest ecosystem restoration. *Appl Environ*
 868 *Microbiol* **83**: 966–983.
- 869 Tateno, R., Hishi, T., and Takeda, H. (2004) Above- and belowground biomass and net primary
 870 production in a cool-temperate deciduous forest in relation to topographical changes in soil nitrogen.
 871 *For Ecol Manage* **193**: 297–306.
- 872 Tatsumi, C., Taniguchi, T., Du, S., Yamanaka, N., and Tateno, R. (2020) Soil nitrogen cycling is
 873 determined by the competition between mycorrhiza and ammonia-oxidizing prokaryotes. *Ecology*
 874 **101**: e02963.
- 875 Tatsumi, C., Taniguchi, T., Du, S., Yamanaka, N., and Tateno, R. (2019) The steps in the soil nitrogen
 876 transformation process vary along an aridity gradient via changes in the microbial community.
 877 *Biogeochemistry* **144**: 15–29.
- 878 Taylor, A.E., Giguere, A.T., Zoebelin, C.M., Myrold, D.D., and Bottomley, P.J. (2017) Modeling of soil
 879 nitrification responses to temperature reveals thermodynamic differences between
 880 ammonia-oxidizing activity of archaea and bacteria. *ISME J* **11**: 896–908.
- 881 Toju, H., Kishida, O., Katayama, N., and Takagi, K. (2016) Networks depicting the fine-scale
 882 co-occurrences of fungi in soil horizons. *PLoS One* **11**: 1–18.
- 883 Toju, H., Tanabe, A.S., Yamamoto, S., and Sato, H. (2012) High-coverage ITS primers for the
 884 DNA-based identification of ascomycetes and basidiomycetes in environmental samples. *PLoS One*
 885 **7**: e40863.
- 886 Torsvik, V. and Øvreås, L. (2002) Microbial diversity and function in soil: from genes to ecosystems.
 887 *Curr Opin Microbiol* **5**: 240–245.
- 888 Tourna, M., Freitag, T.E., Nicol, G.W., and Prosser, J.I. (2008) Growth, activity and temperature
 889 responses of ammonia-oxidizing archaea and bacteria in soil microcosms. *Environ Microbiol* **10**:
 890 1357–1364.
- 891 Trivedi, P., Delgado-Baquerizo, M., Trivedi, C., Hu, H., Anderson, I.C., Jeffries, T.C., et al. (2016)
 892 Microbial regulation of the soil carbon cycle: evidence from gene–enzyme relationships. *ISME J*
 893 **10**: 2593–2604.
- 894 Urakawa, R., Ohte, N., Shibata, H., Isobe, K., Tateno, R., Oda, T., et al. (2016) Factors contributing to
 895 soil nitrogen mineralization and nitrification rates of forest soils in the Japanese archipelago. *For*
 896 *Ecol Manage* **361**: 382–396.
- 897 Urbanová, M., Šnajdr, J., and Baldrian, P. (2015) Composition of fungal and bacterial communities in

- 898 forest litter and soil is largely determined by dominant trees. *Soil Biol Biochem* **84**: 53–64.
- 899 Uroz, S., Oger, P., Tisserand, E., Cébron, A., Turpault, M.-P., Buée, M., et al. (2016) Specific impacts of
900 beech and Norway spruce on the structure and diversity of the rhizosphere and soil microbial
901 communities. *Sci Rep* **6**: 27756.
- 902 Ushio, M., Kitayama, K., and Balsler, T.C. (2010) Tree species-mediated spatial patchiness of the
903 composition of microbial community and physicochemical properties in the topsoils of a tropical
904 montane forest. *Soil Biol Biochem* **42**: 1588–1595.
- 905 Vitousek, P. and Howarth, R. (1991) Nitrogen limitation on land and in the sea: How can it occur?
906 *Biogeochemistry* **13**: 87–115.
- 907 Wan, X., Huang, Z., He, Z., Yu, Z., Wang, M., Davis, M.R., and Yang, Y. (2015) Soil C:N ratio is the
908 major determinant of soil microbial community structure in subtropical coniferous and broadleaf
909 forest plantations. *Plant Soil* **387**: 103–116.
- 910 Wertz, S., Degrange, V., Prosser, J.I., Poly, F., Commeaux, C., Freitag, T., et al. (2006) Maintenance of
911 soil functioning following erosion of microbial diversity. *Environ Microbiol* **8**: 2162–2169.
- 912 Wilhelm, R.C., Singh, R., Eltis, L.D., and Mohn, W.W. (2019) Bacterial contributions to delignification
913 and lignocellulose degradation in forest soils with metagenomic and quantitative stable isotope
914 probing. *ISME J* **13**: 413–429.
- 915 Yao, H., Gao, Y., Nicol, G.W., Campbell, C.D., Prosser, J.I., Zhang, L., et al. (2011) Links between
916 ammonia oxidizer community structure, abundance, and nitrification potential in acidic soils. *Appl*
917 *Environ Microbiol* **77**: 4618–25.
- 918 Zhang, L.-M., Hu, H.-W., Shen, J.-P., and He, J.-Z. (2012) Ammonia-oxidizing archaea have more
919 important role than ammonia-oxidizing bacteria in ammonia oxidation of strongly acidic soils.
920 *ISME J* **6**: 1032–1045.
- 921 Zhu, T., Meng, T., Zhang, J., Zhong, W., Müller, C., and Cai, Z. (2015) Fungi-dominant heterotrophic
922 nitrification in a subtropical forest soil of China. *J Soils Sediments* **15**: 705–709.
- 923
- 924

925 Figure captions

926

927 **Fig. 1** Temporal changes of (a) the net nitrification and (b) the mineralisation potentials of Larch, Fir
928 and Natural forests. The values are means and bars represent the standard deviation. FT, M, and
929 F×M represent the results of the two-way ANOVA for forest types, sampling months, and the
930 interaction of forest type and sampling month, respectively. Symbols represent the following: n.s.
931 represents $p \geq 0.05$ and ** represents $p < 0.01$.

932

933 **Fig. 2** Gene abundances of (a) total bacteria, (b) total archaea, (c) total fungi, (d) AOB, and (e) and
934 AOA. The values are means and the bars represent standard deviations. FT, M, and F×M represent
935 the results of the two-way ANOVA for forest types, sampling months, and the interaction of forest
936 type and sampling month, respectively. Symbols represent the following: n.s. represents $p \geq 0.05$ and
937 *** represents $p < 0.001$.

938

939 **Fig. 3** Predicted counts of genes involved in nitrogen degradation and mineralisation from the
940 rarefied 1441 16S rRNA gene sequences. The values are means and the bars represent standard
941 deviations. FT, M, and F×M represent the results of two-way ANOVA for forest types, sampling
942 months, and the interaction of forest type and sampling month, respectively. Symbols represent the
943 following: n.s. represents $p \geq 0.05$ and * represents $p < 0.05$.

944

945 **Fig. 4** The predicted relative abundances of guilds within the symbiotrophic fungal group. The
946 values are means and the bars represent standard deviations. FT, M, and F×M represent the results of
947 the two-way ANOVA for forest types, sampling months, and the interaction of forest type and
948 sampling month, respectively. Symbols represent the following: n.s. represents $p \geq 0.05$ and ***

949 represents $p < 0.001$.

950

951 **Fig. 5** (a) The co-occurrence network divided by modules, (b) the taxa of the operational taxonomic
 952 units (OTUs) belonging to each module, and (c) the average relative abundance of each module. The
 953 average relative abundances of modules were calculated by summing the average relative
 954 abundances of the OTUs belonging to each module.

955

956 **Fig. 6** The operational taxonomic units (OTUs) with the genes responsible for (a) chitinase, (b)
 957 NAGase, (c) leucine aminopeptidase, (d) arginase, and (e) urease in the co-occurrence network.

958

959 **Fig. 7** The operational taxonomic units (OTUs) with the genes responsible for each nitrification step:
 960 (a) ammonia to hydroxylamine, (b) hydroxylamine to nitrite, and (c) nitrite to nitrate in the
 961 co-occurrence network.

962

963 **Fig. 8** The relationships between the nitrogen mineralisation potentials and (a) the relative
 964 abundances and (b) the estimated absolute abundances of modules 1 to 6. Values in each cell
 965 represent correlation coefficients by Pearson's correlation. Symbols represent the following: n.s., *,
 966 **, and *** represent $p \geq 0.05$, $p < 0.05$, $p < 0.01$, and $p < 0.001$, respectively.

967

968

969

Fig. 1 Nakayama et al.

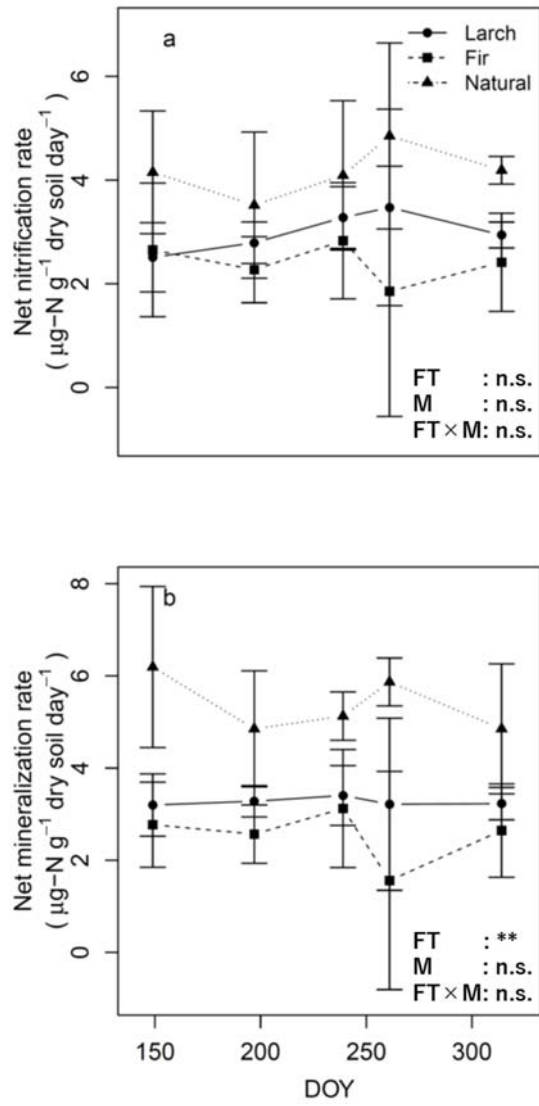


Fig. 2 Nakayama et al.

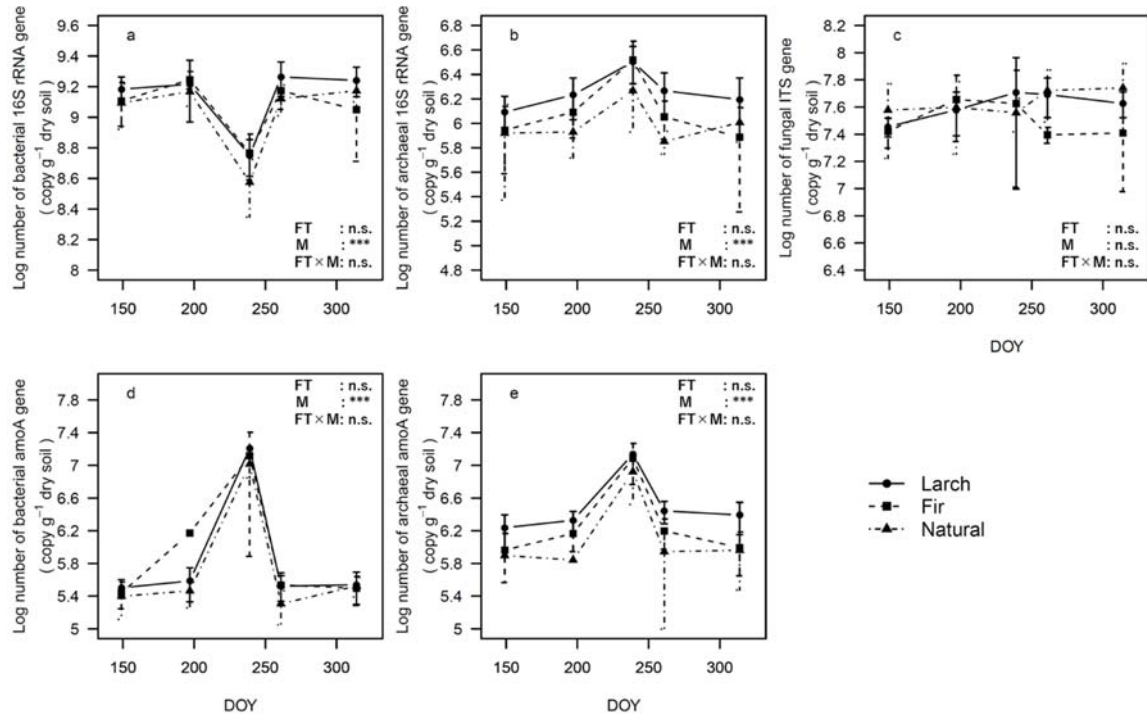


Fig. 3 Nakayama et al.

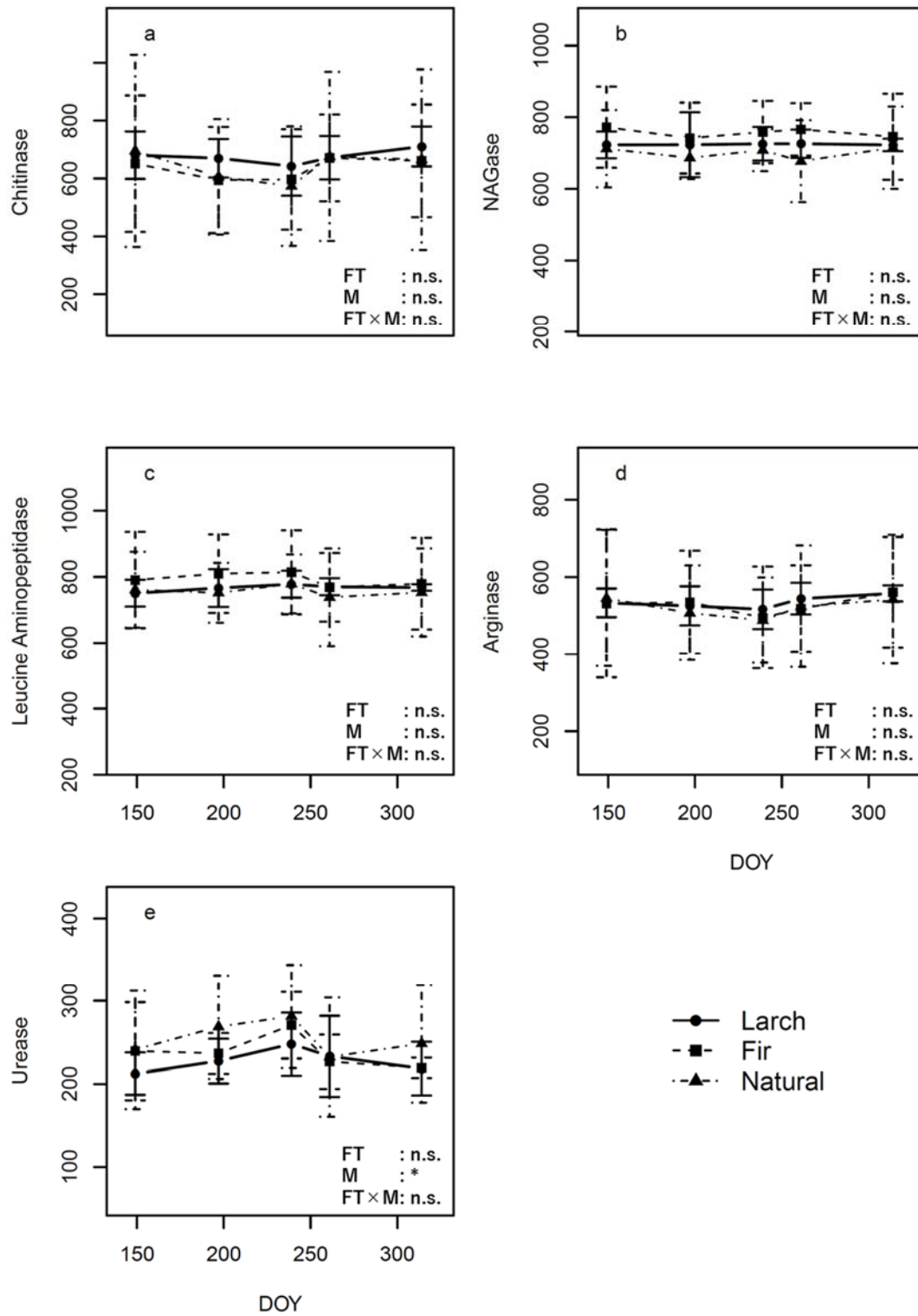


Fig. 4 Nakayama et al.

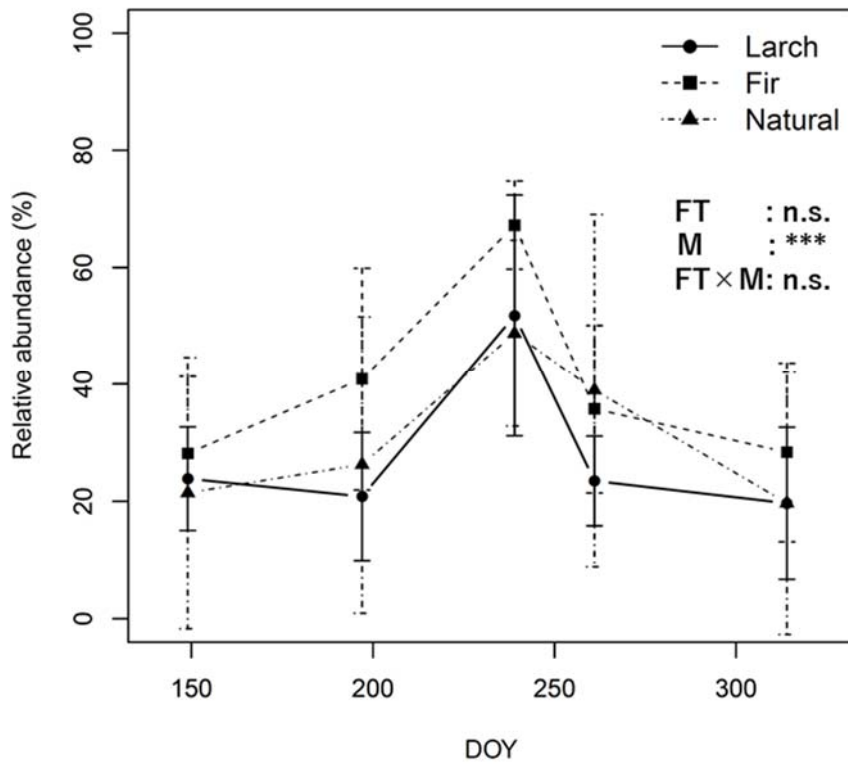


Fig. 5 Nakayama et al.

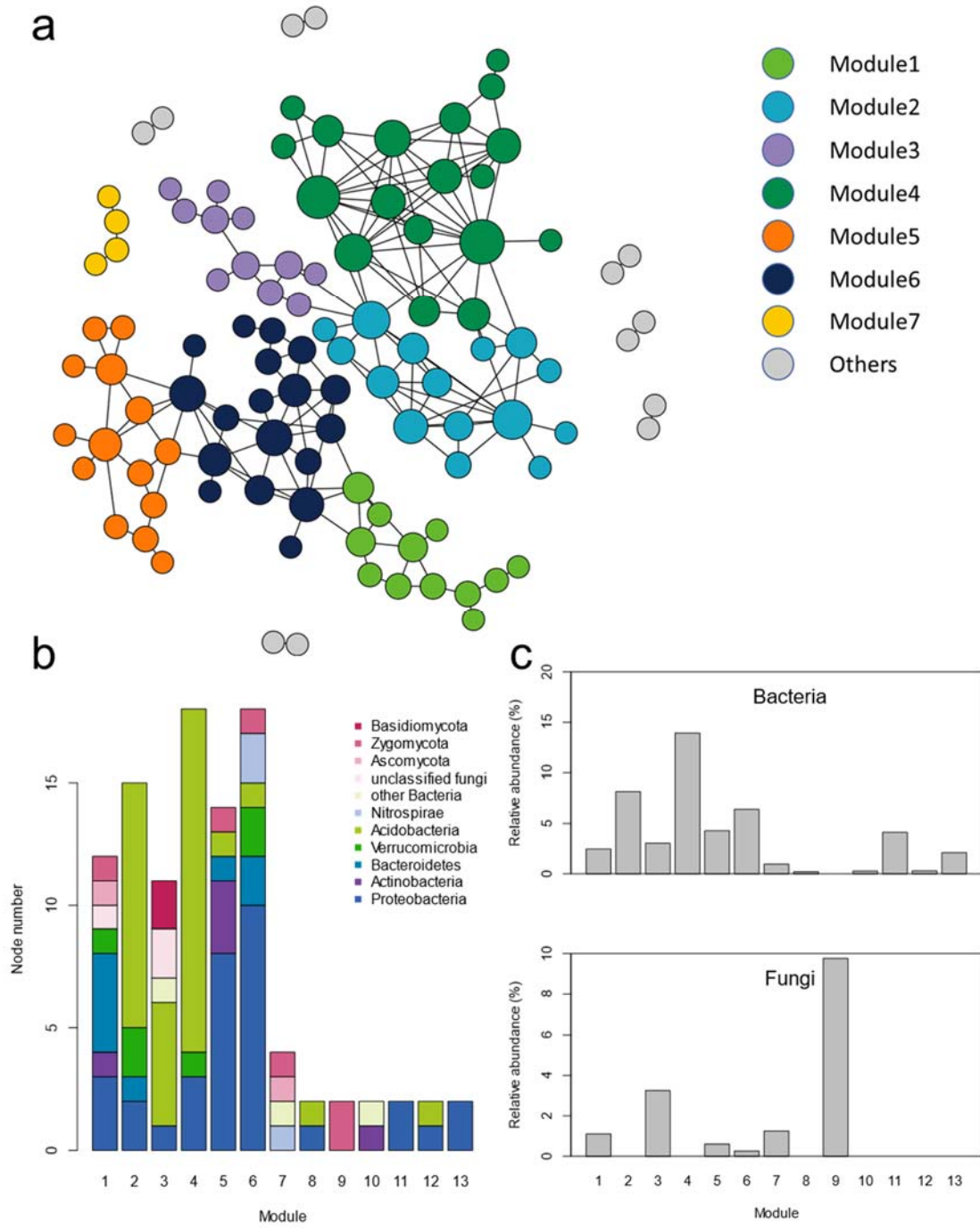


Fig. 6 Nakayama et al.

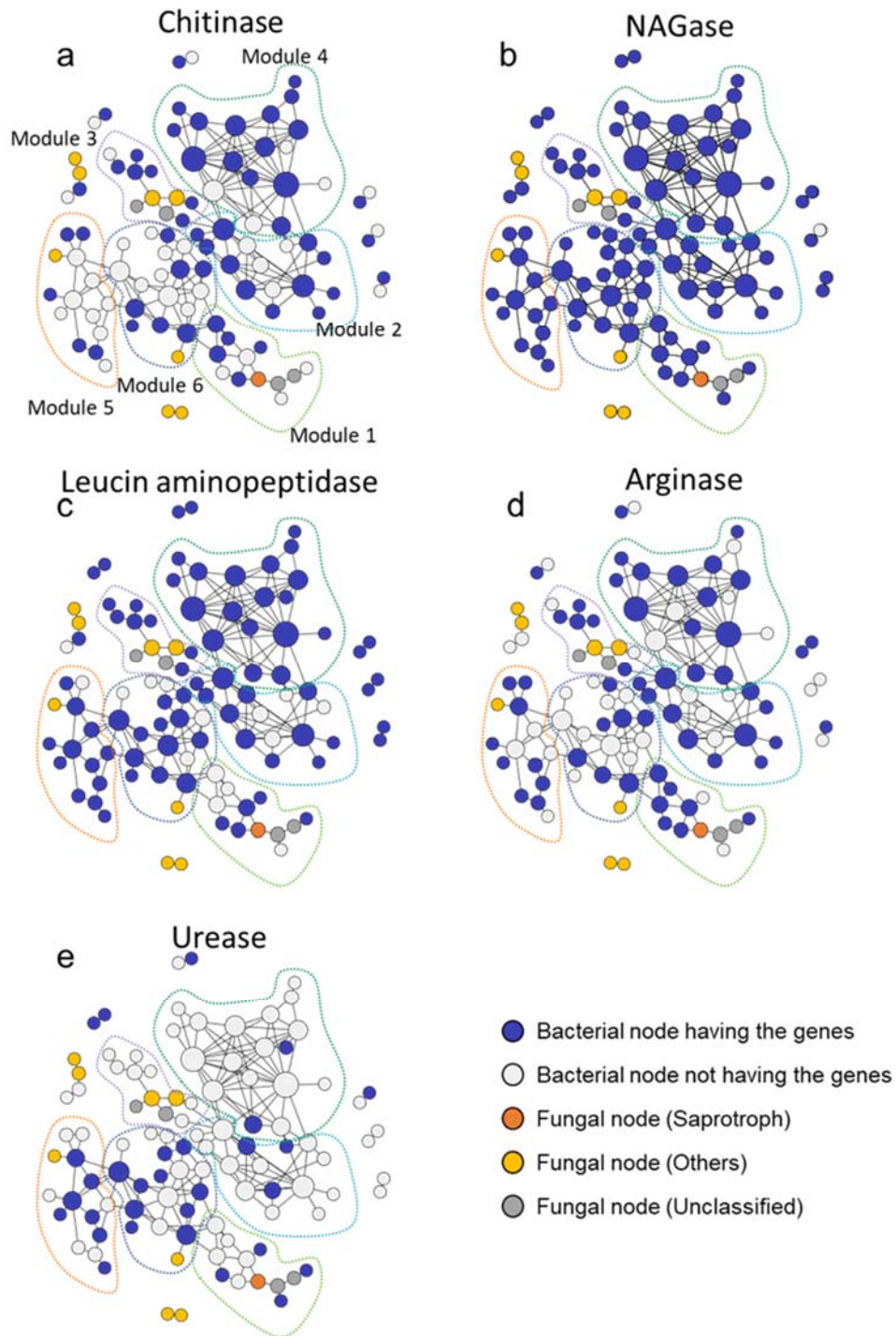


Fig. 7 Nakayama et al.

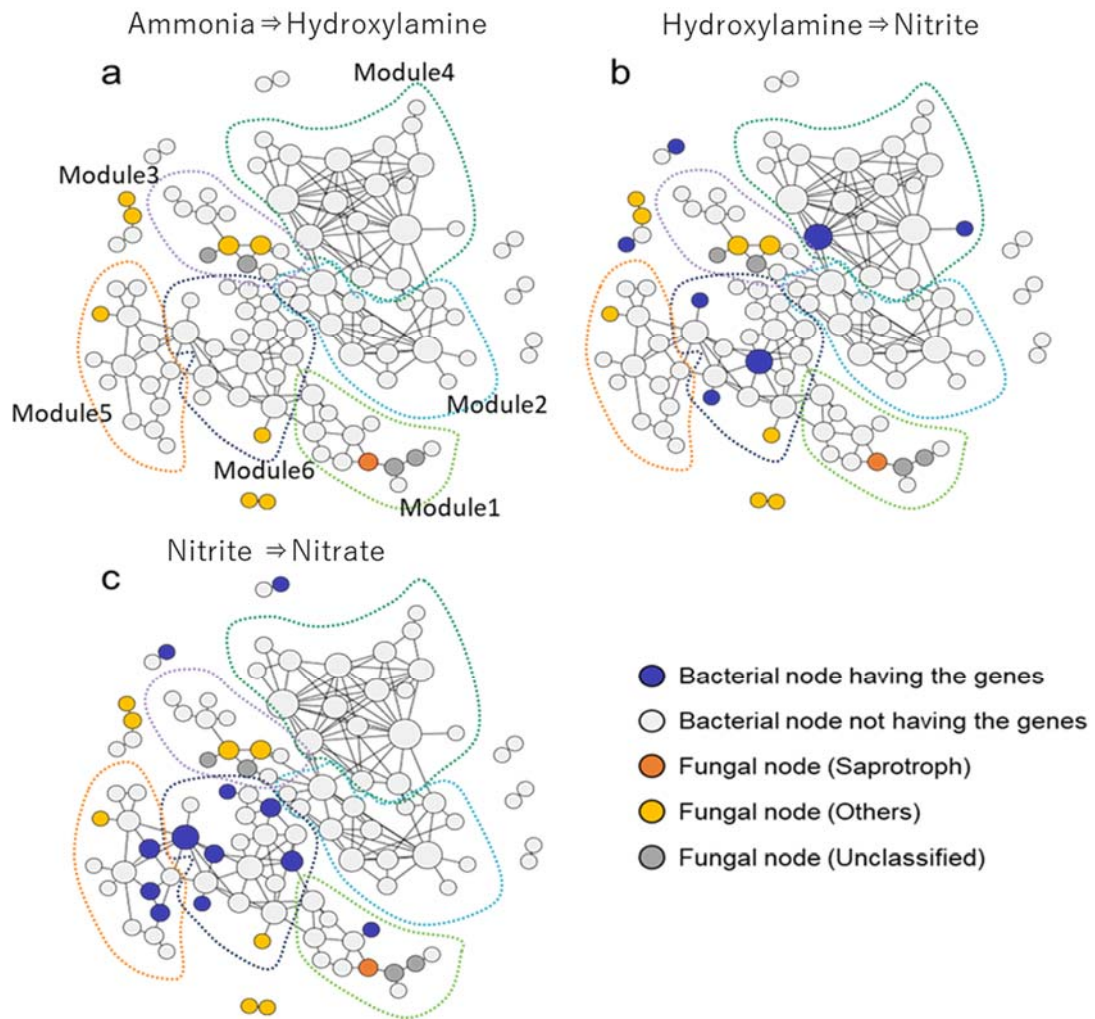


Fig. 8 Nakayama et al.

